

Bringing Anatomical Information into Neuronal Network Models

S.J. van Albada^{1,2}, A. Morales-Gregorio^{1,3}, T. Dickscheid⁴, A. Goulas⁵, R. Bakker^{1,6}, S. Bludau⁴, G. Palm¹, C.-C. Hilgetag^{5,7}, and M. Diesmann^{1,8,9}

¹Institute of Neuroscience and Medicine (INM-6) Computational and Systems Neuroscience, Institute for Advanced Simulation (IAS-6) Theoretical Neuroscience, and JARA-Institut Brain Structure-Function Relationships (INM-10), Jülich Research Centre, Jülich, Germany

²Institute of Zoology, Faculty of Mathematics and Natural Sciences, University of Cologne, Germany

³RWTH Aachen University, Aachen, Germany

⁴Institute of Neuroscience and Medicine (INM-1) Structural and Functional Organisation of the Brain, Jülich Research Centre, Jülich, Germany

⁵Institute of Computational Neuroscience, University Medical Center Eppendorf, Hamburg, Germany

⁶Department of Neuroinformatics, Donders Centre for Neuroscience, Radboud University, Nijmegen, the Netherlands

⁷Department of Health Sciences, Boston University, Boston, USA

⁸Department of Psychiatry, Psychotherapy and Psychosomatics, School of Medicine, RWTH Aachen University, Aachen, Germany

⁹Department of Physics, Faculty 1, RWTH Aachen University, Aachen, Germany

Abstract For constructing neuronal network models computational neuroscientists have access to wide-ranging anatomical data that nevertheless tend to cover only a fraction of the parameters to be determined. Finding and interpreting the most relevant data, estimating missing values, and combining the data and estimates from various sources into a coherent whole is a daunting task. With this chapter we aim to provide guidance to modelers by describing the main types of anatomical data that may be useful for informing neuronal network models. We further discuss aspects of the underlying experimental techniques relevant to the interpretation of the data, list particularly comprehensive data sets, and describe methods for filling in the gaps in the experimental data. Such methods of ‘predictive connectomics’ estimate connectivity where the data are lacking based on statistical relationships with known quantities. It is instructive, and in certain cases necessary, to use organizational principles that link the plethora of data within a unifying framework where regularities of brain structure can be exploited to inform computational models. In addition, we touch upon the most prominent features of brain organization that are likely to influence predicted neuronal network dynamics, with a focus on the mammalian cerebral cortex. Given the still existing need for modelers to navigate a complex data landscape full of holes and stumbling blocks, it is vital that the field of neuroanatomy is moving toward increasingly systematic data collection, representation, and publication.

1 Introduction

Some of the defining characteristics of a neuronal network model are the size of the neuronal populations and the connectivity between the neurons. To determine these properties, the modeler has access to information in multiple forms and based on various experimental methods, where the completeness of the data varies widely across species and brain areas. For instance, the connectivity data for the nervous system of the nematode (roundworm) *C. Elegans* are nearly complete and have enabled full connectomes to be derived with minimal extrapolation from the data [1]. These graphs encode all connections between all of the neurons of the male and hermaphrodite worms. However, the 302 neurons of the hermaphrodite and the 385 neurons of the male worm pale in comparison to larger brains such as the human brain with its roughly 86 billion neurons and trillions of connections. Here, and for most species, measuring a full connectome is still far from feasible in terms of technical and computational effort. For this reason, the anatomical data often need to be complemented with statistical estimates in order to define complete network models of the brain. Filling in the gaps in the known connectivity in this way may be referred to as *predictive connectomics*. The corresponding predictions have to be validated in some way, for instance by leaving out part of the known anatomical data and determining how well these are reproduced by the statistical estimates.

Understanding the human brain is often considered the holy grail of neuroscience, not least because of the hope of finding novel cures and therapies for brain diseases. However, due to its size and enormous complexity, it can be helpful on the way to this goal to investigate simpler, more tractable brains of other species. Eric Kandel took this approach in his famous studies on the sea slug *Aplysia* [2], and it is a guiding thought behind the OpenWorm project on modeling *C. Elegans*. Furthermore, data obtained with invasive methods are, for obvious reasons, much more abundant for non-human brains. Of course, understanding the brains of species besides humans can be seen as a valuable aim in itself—for improving the well-being of animals, for inspiring industrial applications, or as an intellectual pursuit, like cosmology or paleontology, which enriches us culturally even if it has no direct practical application. And, as it is with all basic sciences, one never knows what innovations the knowledge gained may inspire many years into the future. For these reasons, we do not restrict ourselves to the human brain, but also consider various other species. However, we focus on mammalian brains, which exhibit qualitative similarity to the human brain and may therefore teach us most about our own brains. Non-human primate brains deserve particular attention, as they are closest to the human brain in terms of anatomy and function. Although extensive differences in detailed organization remain [3,4,5] the anatomical similarities and evolutionary path give hope that universal principles can be discovered extending to the human brain. Furthermore, the chapter has an emphasis on our study object of choice—the cerebral cortex.

To limit the scope of the chapter, we also restrict ourselves to anatomical properties relevant for networks of point neurons or neural populations, neglect-

ing most aspects of detailed neuron morphology and placement of synapses on the dendritic tree and axonal arborizations. The anatomical characteristics entering into the definition of such neural network models can be classified into brain morphology, cytoarchitecture, and structural connectivity. Brain morphology describes geometric macroanatomical properties, for instance the thickness of the cerebral cortex and its layers, or the curvature. Cytoarchitecture refers to the composition of brain regions in terms of the sizes, shapes, and densities of neurons. Structural connectivity refers to properties of the synaptic connections between neurons, including numbers of synapses between a given pair of neurons, or the probability for neurons from two given populations to be connected.

The type and level of detail of anatomical information that is required depends on the type and aim of the modeling study. A population model, describing only the aggregate activity of entire populations of neurons, does not require the connectivity to be resolved at the level of individual neurons, nor is it generally necessary to know the number of neurons in each population for such models. For models resolving individual neurons, in some cases it may be of interest to incorporate detailed connectivity patterns, while sometimes population-level connection probabilities suffice. The difference lies in the questions that the different types of models allow one to address. In one approach, the modeler tries to derive as realistic a connectivity matrix as possible, in the hope of obtaining the best possible predictions of dynamics and information processing on the anatomical substrate. Here, it always needs to be kept in mind that more detail does not necessarily mean better predictions: adding more parameters can actually reduce the predictive power of a model, for instance when these parameters are not sufficiently constrained [6,7]. However, if this approach is successful, it in principle allows the effects of detailed physiological parameter changes on network dynamics to be predicted (somewhat akin to weather forecasts), which may ultimately find clinical applications. In a contrasting modeling approach, connectivity features are abstracted and the influence of these abstract features (e.g., small-worldness, clustering, hierarchical organization, etc.) on graph theoretical, dynamical, or functional properties of the network are investigated. This approach places less emphasis on strict biological realism and attempts to provide a more conceptual understanding of the links between brain anatomy, dynamics, and function. In practice there is a continuum of approaches between these two extremes. For instance, models may incorporate biologically realistic features at an intermediate level of detail (e.g., population-specific connection probabilities without detailed connectivity at the single-neuron level) in order to simultaneously enable conceptual scientific conclusions and a degree of validation of these conclusions by direct model comparisons with experimental data.

Formulating and parametrizing neuronal network models is still often a painstaking effort, where the researcher digs through a vast literature to collect the relevant parameter values, from disparate experimental methods and labs. This systematization of the available knowledge into a common framework forms a central part of computational modeling work, and allows future researchers to continue at the next level of complexity. It is also highly specific to the modeling

problem and data modalities at hand, so that we cannot give one-size-fits-all advice on how to deal with and interpret anatomical data to develop network models. However, we can provide general guidance regarding what to look out for in the various data modalities, and how to incorporate the corresponding data into models. Furthermore, data are increasingly collected in systematic databases, which make the modeler’s life easier by offering comprehensive data obtained with the same experimental methods, often even from the same lab. Most promising for facilitating this process are recent multilevel brain atlases, which aggregate both macro- and microstructural information into systematic anatomical reference frameworks.

In this chapter, we provide an overview of the types of anatomical information that can be used to define biological neural network models, point to available resources and databases, and describe methods for predicting connectivity and validating the predictions. The text considers physiological properties only where they relate directly to anatomy. This overview is intended as an aid for computational neuroscientists to develop accurate models of biological neuronal networks.

2 Brain morphology and cytoarchitecture

In this section, we describe the main types of information on the morphology and cytoarchitecture of brain regions, and corresponding resources available to modelers. We start by providing a brief introduction to brain atlases, which systematize information on these anatomical properties. Next, we treat the morphological property of cortical and laminar thicknesses in more detail. We then go into the determination of neural population sizes and the location of neurons within brain regions, and close with a short discussion of the use of morphology and cytoarchitecture in computational models. We do not distinguish between cell types within regions, as this would substantially extend the scope of the chapter, and, especially in the context of network models that do not resolve neural compartments, more directly concerns chemical and electrophysiological instead of anatomical properties.

2.1 Brain atlases

Brain atlases are a tool for defining brain areas and aggregating regional descriptions of the brain in a consistent anatomical framework. A brain atlas typically consists of a template space, a set of maps or a parcellation, and a taxonomy, which provides the names and mutual relationships of those regions.

The template space of a brain atlas is typically represented by one or multiple scans of a brain, which provide an anatomical description of an underlying standardized coordinate space. Depending on the task at hand, different template spaces are used. A classical template space for the human brain is Talairach space [8], which assumes that the relative distances between brain regions are

preserved between individuals, and defines a rescalable grid accordingly. Talairach coordinates are still in wide use in functional neuroimaging. Today, it is more common to use one of the MNI templates defined by the Montreal Neurological Institute [9,10], which include single- and multi-subject averages of MRI scans as volumetric standard spaces. While the MNI templates define standard spaces at millimeter resolution, the BigBrain offers a brain model of a single subject based on a three-dimensional reconstruction from 7,400 histological sections, at an isotropic resolution of $20\ \mu\text{m}$ [11]. As the tissue sections were stained for cell bodies, this model provides the most detailed three-dimensional reference of human cytoarchitecture available today. Ongoing research addresses the three-dimensional cellular-level reconstruction of brains at $1\ \mu\text{m}$ resolution, which poses considerable technical challenges for human brains due to their size and topological complexity [12].

Brain maps and parcellations assign brain regions to coordinates of a template space. In case of a standard whole-brain parcellation, each voxel has a unique region index, and the assigned regions do not overlap. In case of probabilistic maps, however, each coordinate is assigned a probability to belong to any of the regions, resulting in a set of overlapping maps to define the atlas. Parcellations are based on different modalities of brain organization, including cytoarchitecture (e.g. [13]), chemoarchitecture (spatial distribution patterns of molecules like specific neurotransmitter receptors, e.g. [14]), structural connectivity (patterns of connectivity with other brain regions as defined by axonal connections, e.g. [15,16]), functional connectivity (spatial co-activation patterns under different cognitive conditions (e.g. [17]), anatomical landmarks, or a combination of such features in the case of multimodal parcellations [18,19,20].

The gold standard of brain parcellations is based on cytoarchitecture as measured in histological sections. The early Brodmann atlas of the cerebral cortex of humans and other primates uses such a cytoarchitectonic parcellation [21]. Some years later, von Economo and Koskinas developed an atlas [22] with a more comprehensive characterization of the cortical layers, and taking into account cortical folding by describing cytoarchitecture orthogonal to the cortical surface. However, the bases of these pioneering works remain collections of separate brain slices, thereby lacking coverage of the full three-dimensional anatomical space, as well as of the variability across subjects. Recent work in probabilistic cytoarchitectonic mapping addresses the latter challenge by aggregating microscopic maps from ten different subjects in MNI space [13]. Furthermore, different groups are working on full three-dimensional, microscopic resolution maps of cytoarchitectonic areas [23] and cortical layers [24] in the BigBrain model, giving access to region- and layer specific measures of, e.g., cell densities and laminar thickness.

In connectivity-based parcellation, voxels with similar connection properties are grouped together [15]. An example of an atlas using connectivity-based parcellation is the human Brainnetome Atlas [16], which takes the Desikan-Killiany atlas based on cortical folds (the sulci and gyri) [25] as its starting point. The Brainnetome atlas has the advantage for modeling studies that data on functional connectivity, a term used in neuroscience for activity correlations, is freely

available in the same parcellation, allowing straightforward testing of model predictions on network dynamics.

The Allen Institute has published multiatlases of the developing¹ and adult human brain [26,27], mapping cytoarchitecture, gene expression, and for the adult brain also connectivity as measured with diffusion tensor imaging (DTI), a magnetic resonance imaging method that detects axon tracts. This multimodality, where different types of data are represented in the same template space and parcellation, is useful for modelers, not only because of the richness of the data, but also as mapping data from different sources between template spaces and parcellations introduces inevitable errors.

The macaque, as a close relative of humans, is an important model organism, for which several atlases have been created. These include the atlas of Markov et al. (2014) [28] with the so-called M132 parcellation of 91 cortical areas, and a whole-brain atlas by Calabrese et al. (2015) [29] based on DTI. Another commonly studied species is the mouse, for which state-of-the-art atlases of gene expression data [30], cytoarchitecture as measured with Nissl staining, which stains nucleic acids and thereby cell bodies of both neurons and glia, and mesoscopic connectivity obtained by anterograde viral tracing [31,32] are provided by the Allen Institute. Paxinos and Franklin provide the other most commonly used mouse brain atlas [33], which recent work combines with the Allen Institute coordinate framework [34].

Several online resources exist for browsing brain atlases. The Scalable Brain Atlas provides web-based access to a collection of atlases for the human brain and for a number of other mammals, including macaque, mouse, and rat [35]. The Human Brain Project provides online services for interactive exploration of atlases for the mouse, rat, and human brain through the EBRAINS infrastructure². The human brain atlas is a multilevel framework based on probabilistic atlases of human cytoarchitecture, and includes links with maps of fiber bundles and functional activity, as well as a representation of the microscopic scale in the form of the BigBrain model with maps of cortical layers and cytoarchitectonic maps at full microscopic resolution [36].

2.2 Cortical and laminar thicknesses

The geometrical properties of the global and regional morphology of the brain have obvious relevance for brain models that explicitly represent space, but can also be important for estimating connectivity and numbers of neurons in non-spatial models. These properties include coordinates of region boundaries, spatial extents of brain regions, and properties of regional substructures such as thicknesses of cortical layers. Coordinates and spatial extents of brain regions are captured by atlases as described in the previous section. Another geometric property that is often of interest is the thickness of cortex and its layers.

¹ BrainSpan Atlas of the Developing Human Brain (2011) <http://brainspan.org>. Funded by ARRA Awards 1RC2MH089921-01, 1RC2MH090047-01, and 1RC2MH089929-01.

² <https://ebrains.eu/services/atlas/brain-atlas>

Cortical and laminar thicknesses can be either determined directly from histology of brain slices, or using structural MRI. When the MRI scans have sufficiently high resolution, these methods yield comparable results [37,38,39,40], but both methods have their own drawbacks. Brain slices generally represent sparse samples, are difficult to obtain precisely perpendicularly to the cortical sheet, and are subject to shrinkage, which has to be controlled for. Furthermore, identification of layers and the boundary between gray and white matter is still often performed manually, although automatic procedures are under development [24,41]. Structural MRI can cover the entire cortex and at least the gray/white matter boundary tends to be segmented using computer algorithms, but it has a lower resolution in the section plane than microscopy of brain slices, the exact resolution depending on the strength of the scanner and the scanning protocol. Von Economo provides laminar and total cortical thicknesses for all areas of human cortex based on $25\ \mu\text{m}$ sections [42]. More recently, cortical and laminar thicknesses (the thicknesses of the individual cortical layers) have been identified in the BigBrain, forming a state-of-the-art, comprehensive dataset on human cortex [24,43]. The gray and white matter volumes and surfaces, along with the layer surfaces, are freely available³ and can be explored interactively in the EBRAINS human brain atlas viewer. Alvarez et al. (2019) [44] determined the thicknesses of 25 human visual areas from $700\ \mu\text{m}$ resolution MRI data from the Human Connectome Project, also making the quantitative area-averaged data freely available. Calabrese et al. (2015) [29] derived macaque cortical thicknesses from MRI scans at $75\ \mu\text{m}$ resolution, available as an image file. Hilgetag et al. (2016) [45] provide total cortical thicknesses for 22 vision-related cortical areas of the macaque monkey, determined from brain slices sampled every $150\text{--}200\ \mu\text{m}$ throughout the region of interest. At least in the vision-related areas of macaque cortex, total cortical thickness correlates inversely with neuron density, so that a statistical fit allows the thicknesses of the remaining vision-related areas to be estimated [46]. Correspondingly, cortical thickness varies systematically along the anterior-posterior axis in primates [47]. Rough estimates of the laminar thicknesses of macaque vision-related areas based on a survey of micrographs (microscopic images) have been published [46]. Comprehensive data on cortical thicknesses of other species are sparse, especially in a form that is directly usable by modelers. Methods for extracting cortical thicknesses from MRI in rodents are under development [48,49].

2.3 Numbers of neurons

Another basic property of brain circuits is their numbers of neurons, which can be determined from the size of brain regions and their neuron density. Over the years, different methods of counting cells have been used [50,51]. When total cell counts are of interest and their precise distribution across space is less important, tissue can simply be homogenized and the numbers of cell nuclei suspended in a fluid can be counted in samples under a microscope. The isotropic fractionator

³ <ftp://bigbrain.loris.ca/>

is a version of such a homogenization and direct counting method [52]. The term ‘fractionator’ refers to a uniform random sampling scheme which divides samples into ‘fractions’ or counting boxes, enabling a statistical estimate of total cell counts to be obtained by considering only some fractions [53].

Stereological methods are a more involved class of methods that determine three-dimensional properties from two-dimensional sections through the tissue. The advantage of these methods is that the cells are counted in their real three-dimensional environment (depending on the section thickness) and thus spatial and area-specific values can be collected, e.g. cell densities in a single cortical lamina. Beside the fact that most stereological methods are quite labor- and time-intensive, the problem arises that the same cell may appear in two or more sections but should only be counted once. The disector addresses this issue by considering pairs of adjacent sections and only counting the cells that are present in the second but not the first section, effectively counting only the ‘tops’ [54]. The success of this approach depends on being able to recognize if features in the adjacent sections belong to the same cell, and on effectively correcting for large structures that extend across more than two sections. The optical fractionator combines the aforementioned uniform sampling method (the ‘fractionator’) with optical dissection, in which objective lenses with a high numerical aperture are used to focus through the tissue to identify individual cells. A guarding zone above and below the inspected volume prevents multiple counting of truncated structures.

For cell bodies to be identified under the microscope, they are first dyed. Two commonly used methods are the aforementioned Nissl staining, and antibody staining of the protein NeuN that is present in the nuclei of most vertebrate neurons but not in glia [55]. Another technique dyeing both neurons and glia is silver staining [56], used for instance in the BigBrain model.

A number of comprehensive data sets on cell and neuron counts are available, although estimates can vary quite a bit across studies [57]. Overall numbers of neuronal and non-neuronal cells have been estimated for the brain as a whole, and for its major components like the cerebral cortex and the cerebellum, for a large number of species⁴ [58,59,60,61,62]. In most cases, these cell numbers were acquired using the above-described techniques based on homogenized tissue. The von Economo atlas contains cell densities for human cortex with areal and laminar resolution, as determined with Nissl staining [42]. Because the Nissl technique stains both neurons and glia, which can, however, be distinguished based on morphology, it is not entirely clear whether glia are included in these cell densities. Furthermore, the cell numbers were measured without modern stereological approaches and without characterizing inter-individual variability. Modern high-performance computing methods are being applied for image registration of two-dimensional cortical and subcortical images to determine three-dimensional cell distributions [12] (figure 1), laying the foundation for future quantitative data sets representing an update and refinement with respect to the von Economo study. Collins et al. [63] provide cortical area-specific neuron

⁴ https://en.wikipedia.org/wiki/List_of_animals_by_number_of_neurons

densities for the non-human primates galago, owl monkey, macaque, and baboon as determined with the isotropic fractionator. So-called cortical types or architectural types characterize the neuron density and laminar differentiation of primate cortical areas in a discretized manner, and thereby enable rough neuron density estimates where these have not been directly measured [64,65,46,66,67]. Herculano-Houzel et al. (2013) [68] measured neuron and cell counts and densities for the areas of mouse isocortex. Keller et al. (2018) [69] systematically reviewed region-specific neuron and glial densities throughout the mouse brain. Structures that have been characterized in detail also include the somatosensory areas of rat cortex and thalamus [70,71]. Despite many more data having been published, a large number of species-specific brain region compositions are still unknown, especially for subcortical regions. Scaling laws across species enable numbers of neurons to be estimated based on structural properties like brain and regional mass and volume [72,58,59,60,61,62].

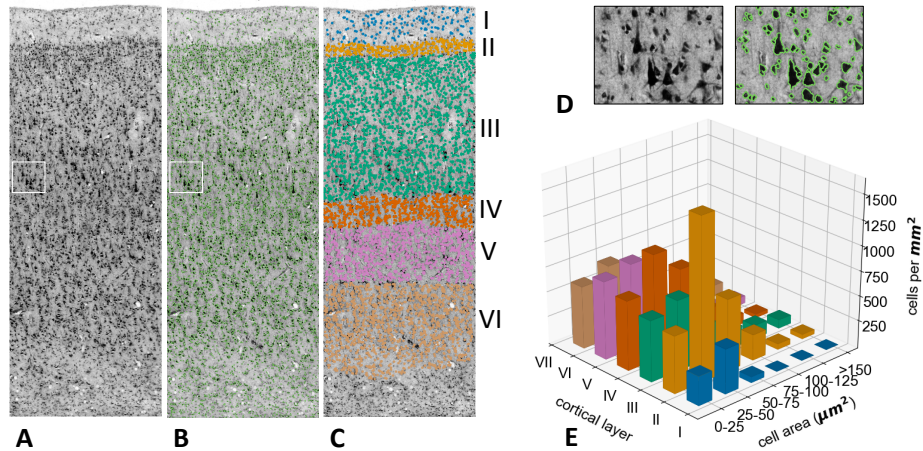


Figure 1. Extraction of layer-specific cell density estimates from microscopic scans of histological sections stained for cell bodies. **A.** Cortical patch of a scan. **B.** Example result of automatic instance segmentation of cell bodies using state-of-the-art image analysis (E. Upschulte, Institute of Neuroscience and Medicine, Forschungszentrum Jülich). **C.** Centroids of detected cell bodies, colored by cortical layer. **D.** Zoom into the local region of interest indicated by the white rectangle in Panels A and B. **E.** Two-dimensional histogram showing the number of cells in each layer, grouped by area of the cell body as segmented in the image.

Neuron counts or densities may not always be available in the particular parcellation chosen by the modeler. A mapping between parcellations may be performed by determining the overlaps between areas in different parcellations, for which the parcellations have to be in the same reference space. A large number of methods for registering images to the same reference space using nonlinear

deformations have been developed [73,74,75]. For macaque atlases registered to the so-called F99 surface, a tool provided alongside the CoCoMac database on macaque brain connectivity⁵ [76] calculates the absolute and relative overlaps between cortical areas. The data in the new parcellation can then be computed as a weighted sum over the contributions from the areas in the original parcellation. However, this method entails the assumption that the anatomical data for each given area are representative of that area as a whole, and neglects inhomogeneities within areas. It should further be noted that criteria for area definitions, such as their cytoarchitecture or connectivity, are likely to provide information beyond this purely spatial approach. Nonlinear image registration techniques can take such factors into account, or alternatively, a coordinate-independent mapping can be performed [77]. No perfect solution for mapping anatomical data between parcellations exists, but in general, the more criteria are considered, the better the mapping.

2.4 Local variations in cytoarchitecture

Even within brain regions, cell densities are not constant but display local variations. An example of known spatial organization of neuron positions are so-called cortical minicolumns, also known as microcolumns, arrangements of on the order of 100 neurons perpendicular to the cortical surface, across the cortical layers. Cortical macrocolumns or hypercolumns are millimeter-scale structures containing thousands or tens of thousands of neurons with similar response properties in one or a few coding dimensions, for instance ocular dominance or position in the visual field. Cortical macrocolumns are particularly pronounced in the barrel cortex of rodents, which encodes whisker movements. In barrel cortex, the ‘barrels’ are cylindrical structures in layer IV containing neurons that respond preferentially to a particular whisker and have response properties and connectivity distinct from the interbarrel regions.

Various data on variations in neuron density within brain regions are available. Probably the most comprehensive data set of three-dimensional cell distributions is the Allen Mouse Brain Atlas, which contains both neurons and glia [57]. Spatial gradients in retinal cell densities have been well characterized [78,79,80,81,82,83], and those in thalamus to a lesser extent (e.g., [84]). The vertical distribution of cells in several cortical areas has also been characterized at a spatial resolution beyond that of cortical layers [85,86,87].

Studies resolving small cortical patches provide a sense of the variability of neuron density across the cortical sheet within primate cortical areas [63,88]. Furthermore, many studies have subdivided brain regions into discrete components with different cellular compositions, e.g., [89,90,91,92].

2.5 Use of morphology and cytoarchitecture in models

While most neural network models specify their architecture using concepts such as areas and layers, in some cases the neurons are simply assigned positions in

⁵ http://cocomac.g-node.org/services/f99_region_overlap.php

continuous three-dimensional space and the connectivity is specified without reference to such concepts (e.g. [93]). In the conceptual approach, different connectomes may be obtained depending on the chosen parcellation. The particular choice of parcellation for instance affects topological properties of the corresponding connectomes [94,95]. Apart from this ‘gerrymandering’ issue, when predictive connectomics is used to fill in gaps in connectivity data with the conceptual approach, the choice of parcellation may influence the results. The findings of [94,95] for instance imply that incomplete connectomes completed via topological rules could differ depending on the parcellation. In view of the variability induced by differences between parcellations, there is something to be said for the continuum approach when the data allow it. Interpretation of the network dynamics in terms of region-specific activity may then be done in a post-hoc manner, flexibly with regard to the region definitions.

In spatially extended models, the neurons may be placed on a regular grid, with some jittering, at random positions, or at precise coordinates in space. Here, artificial symmetries in the network dynamics due to grid-like placement of neurons, which may arise for instance when the connectivity and delays are directly determined by the distances between neurons, should be avoided. Besides informing connectivity, the positions can be important for predicting signals with spatial dependence, like the local field potential (LFP), electroencephalogram (EEG) or magnetoencephalogram (MEG).

Precise region shapes are so far hardly used in computational modeling. Rather, the relatively rare network models that take into account three-dimensional structure tend to restrict themselves to simple geometric shapes like cubes or cylinders. An available but not yet widely used tool enables three-dimensional region volumes to be modeled through a combination of deformable two-dimensional sheets, where atlas data or histological images can support the modeling process via integration with the software Blender [96]. In an example application, the three-dimensional shape of the hippocampus was shown to substantially affect the connectivity between neurons predicted based on their distance. Accurate representations of volume transmission effects such as ephaptic coupling (non-synaptic communication via electrical fields or ions) [97], as well as the prediction of meso- and macroscopic signals like the LFP, EEG, and MEG also rely on the spatial distribution of neurons and thus benefit from measured three-dimensional brain morphology [98,99,100].

On the scale of local microcircuits on the order of a millimeter, spatial variations in cortical and laminar thicknesses across the cortical sheet within each area are limited and are generally ignored in computational models. Cortical and laminar thicknesses are then straightforwardly incorporated by scaling the numbers of neurons accordingly, and sometimes by distributing the neurons across cortical depth. In future, as resources become available for modeling extended cortical regions in detail, continuous variations in cortical and laminar thicknesses may be incorporated.

It is also not yet common for computational models to take into account continuous variations in neuron density within brain regions. However, a number

of models already divide regions into discrete subdivisions with different cellular compositions, e.g., [101]. The organization of cortex into minicolumns and macrocolumns has been incorporated for instance in models of attractor memory [102,103] motivated by a functional interpretation. In future, increasingly realistic placement of neurons in models may yield more sophisticated predictions of spatially resolved brain signals and of network dynamics, through associated properties like distance-dependent connectivity.

3 Structural connectivity

Neurons in the brain exchange chemical signals via synapses, and in some cases are in more direct contact via so-called gap junctions. Although gap junctions are probably important for some phenomena (e.g. [104]), we here focus on the former, much more numerous type of connections, the synapses. The huge number of synapses in mammalian brains has so far precluded mapping all of them individually, although efforts are underway towards dense reconstruction of the mouse brain [105]. However, various methods exist for measuring neuronal connectivity, at scales ranging from individual synapses to entire axon bundles between areas. While some models distinguish individual synapses and thus need information at this level, other models lump synapses together, so that aggregated connectivity information suffices.

This section provides an overview over available types of information on neuronal network connectivity, along with resources and databases that can be used for constructing neuronal network models. We describe connectivity information according to the major experimental methods: microscopy, paired recordings, glutamate uncaging, axonal tracing, and diffusion magnetic resonance imaging (diffusion MRI), of which the most commonly used form is diffusion tensor imaging (DTI).

3.1 Microscopy

The oldest and lowest-resolution form of microscopy is light microscopy, providing a magnification factor of up to about 1,000. Neuron reconstructions from light microscopy of adjacent tissue slices allow rough estimates of connectivity based on the proximity of pre- and postsynaptic neural processes (cf. section 4.1). Following this approach, Binzegger et al. (2004) [106] derived a population-level local connectivity map for cat primary visual cortex. However, as detailed in section 4.1, predicting connectivity based on proximity has its drawbacks, which should be kept in mind when interpreting the resulting connectomes. Furthermore, tissue slicing cuts off dendrites and axons, which may extend over millimeters and more, so that assessing medium- to long-range connectivity requires extensive three-dimensional reconstructions. A method that facilitates such reconstructions is block-face tomography, in which scanning of the surface of a tissue block is alternated with the removal of thin slices from the surface [107].

Two-photon microscopy is a sub-micron resolution imaging technique that uses laser irradiation of tissue to elicit fluorescence through two-photon excitation of molecules [108]. A high-throughput block-face tomography pipeline has enabled the reconstruction of the full morphologies of 1,000 projection neurons in the mouse brain at a resolution of $0.3 \times 0.3 \times 1 \mu\text{m}^3$, the MouseLight data set of Janelia Research Campus [109,110]. A viewer for the MouseLight morphologies is available⁶. A finding that stands out from this data set is the remarkable variability in projection patterns, each neuron projecting to a different subset of target regions for the given source region.

At nanometer spatial scales, electron microscopy enables the identification of individual synapses and the precise shape and size of the presynaptic and postsynaptic elements, even down to individual synaptic vesicles. This method is extremely labor-intensive, but heroic efforts have nevertheless led for instance to estimates of synapse density in different areas of human cortex [111,112], a volume reconstruction of the entire *Drosophila* (fruit fly) brain [113], the morphological reconstruction of 1,009 neurons in a microcircuit of rat somatosensory cortex [71], and full reconstructions of $1,500 \mu\text{m}^3$ [114] and more recently $> 5 \times 10^5 \mu\text{m}^3$ [115] of mouse cortical tissue. A noteworthy finding from these studies is that the presence of synapses is not perfectly determined by the close proximity of axons and dendrites (appositions). For instance, an apposition is far more likely to predict an actual synaptic contact for pairs of neurons that also form synapses elsewhere on the axon and dendrite [114]. Such a rule will tend to lead to a long-tailed distribution of the multiplicity of synapses between pairs of neurons.

Synapses may look asymmetric or symmetric under the microscope, where asymmetric synapses have a pronounced postsynaptic density and are predominantly excitatory, while symmetric synapses have roughly equally thick pre- and postsynaptic densities and tend to be inhibitory. Both the size of synapses and their location on dendrites are informative about their effective strength in terms of postsynaptic potentials evoked at the soma [116,117,118,119]. Furthermore, synapse locations on dendrites can tell us something about their interaction with other synapses; however, these complex interactions are not captured by point neuron or population models. Axonal varicosities or boutons are swellings along axons (boutons en passant) or at axon terminals (terminal boutons) that host synapses, and which are detectable through all microscopic methods mentioned here. Even when the synapses themselves are not directly imaged, boutons may be taken as evidence for synapses, with the caveats that some synapses are not established on boutons, and individual boutons may contain different numbers of synapses [120].

In summary, microscopy is useful for estimating connectivity based on appositions, reliable estimates of numbers of synapses in a given volume, detailed connectivity features such as the multiplicity of synapses between pairs of neurons, and correlative information on synaptic efficacy.

⁶ <https://neuroinformatics.nl/HBP/mouselight-viewer/>

3.2 Paired recordings

In paired recordings, electrodes are used to simultaneously stimulate one cell and measure the response in another cell, either *in vitro* or *in vivo*. Stimulation may be performed extracellularly, intracellularly with sharp electrodes, or via patch clamp; recordings normally use one of the latter two techniques. This method sums up the contributions from potentially multiple synapses between the pair of neurons, which should be kept in mind when incorporating the corresponding synaptic strengths into models. Where anatomy-based methods can have the drawback that they do not provide conclusive evidence for physiologically active synapses, paired recordings identify functional synapses. However, existing connections may be missed depending on the experimental protocol, for instance due to axons and dendrites being cut off during slice preparation. Each pair of neurons should also be tested multiple times, because in individual trials, axonal or synaptic transmission failures may occur, or the postsynaptic potential may be too small to be detectable among the noise [121]. Paired recordings may be biased toward neurons that are easier to patch or insert an electrode into, for instance larger cells. Especially *in vivo*, where the network exhibits background activity, responses may in principle be caused by activation of neurons other than the one that is stimulated. Responses are judged to be monosynaptic based on a short, consistent response latency, usually of a few tenths of milliseconds [122,123].

Most paired recordings are highly local, with a distance no greater than $100\ \mu\text{m}$ between the somas of the pre- and postsynaptic cells. They provide the modeler with connection probabilities in terms of the fraction of pairs of neurons that have at least one synapse between them. For interpreting these connection probabilities, it is important to take into account the spatial range of the recordings, as connection probability is generally distance-dependent. The measurements represent a spatial average over this distance-dependent connectivity, which is in mathematical terms a double sum (which may in continuum approximation be represented by an integral) over the positions of the source and target neurons.

Paired recordings show that, on the scale of local microcircuits up to $200\ \mu\text{m}$ from the presynaptic soma, bidirectional connections between pyramidal neurons in cortical layer V occur significantly more often than would be expected by chance [124]. In some studies, researchers have recorded from multiple neurons simultaneously [125,126,127,128]. Simultaneous recordings from respectively four [126] and twelve [127] rat cortical neurons confirm the overrepresentation of bidirectional connections regardless of the distance from the soma. This type of analysis has also revealed that motifs with clustered connections among three or more neurons are more common in the cerebral cortex than would be predicted based on pairwise connection probabilities alone [126,127] (cf. section 4.4).

3.3 Glutamate uncaging

Similarly to paired recordings, glutamate uncaging generates action potentials in presynaptic neurons and records the response in postsynaptic neurons con-

nected to them. Usually, the method is applied to slice preparations and neurons are recorded intracellularly, but *in vivo* application and extracellular recordings are also possible. First, a compound consisting of glutamate bound to another molecule is introduced, for instance by bathing a brain slice in a solution with the caged glutamate. Then glutamate is released by photolysis of the compound through focal light stimulation, causing action potentials in neurons with their soma close to the stimulation site. Brain slices are generally scanned systematically, generating for each given target neuron a grid-like map of response amplitudes for each stimulated location.

Originally, glutamate was uncaged using ultraviolet light [129], but due to light scattering and a large uncaging area, this stimulated multiple neurons, making the results harder to interpret. Two-photon stimulation, in which photolysis is triggered by the absorption of two photons, enables individual neurons and even individual dendritic spines to be stimulated [130,131]. As with paired recordings, an issue is that it cannot be known with certainty whether the responses are monosynaptic or emerge due to sequential activation of two or more neurons, but short-latency responses time-locked to presynaptic action potentials in the absence of background activity reliably indicate monosynaptic connections. Another issue is that the uncaged glutamate may directly influence the recorded neuron, so that stimulations that lead to short-latency responses with excessive amplitudes have to be excluded from analysis. Furthermore, the same caveats as for paired recordings apply with regard to distance dependence of connectivity, and potential cutting of dendrites and axons during slice preparation.

Purely based on glutamate uncaging response maps, it is not possible to directly derive a neuron-level connectivity map, because it is unknown how many different presynaptic neurons are activated across stimulation sites. However, by combining glutamate uncaging with imaging of the neurons, the connectivity between neurons can be determined [130]. In the absence of such direct imaging, the number of source neurons eliciting a given glutamate uncaging response can be estimated by dividing by the unitary synaptic strength (the PSP or PSC size due to a single presynaptic neuron), if an independent estimate for the latter is available. If one in addition makes an assumption about the average number of sites from which a given presynaptic neuron is activated, which depends on the resolution of the stimulation grid, this yields an estimate of the number of neurons impinging on a given postsynaptic cell. Typically, action potentials can be elicited in a given neuron from a handful of sites [132,133]. Finally, one can derive a connection probability by dividing by the approximate number of neurons in the stimulated volume. Clearly, many assumptions and approximations are involved in such derivations, so that it is currently still difficult to reliably determine the connectivity of neural network models from glutamate uncaging data. However, in some cases, data obtained by this method are the best available for a given brain region, in which case one may proceed via such assumptions [134].

3.4 Axonal tracing

The technique of axonal or neuroanatomical tracing entails injecting a tracer, which can be a molecule or virus, which is taken up by neurons and transported toward cell bodies or axon terminals. In anterograde tracing, the tracer is transported in the forward direction toward the synapses, while in retrograde tracing, it is transported in the backward direction from axons toward the cell bodies of the sending neurons. In practice, most tracers are to some extent both anterograde and retrograde, but one transport direction dominates [135]. Detection of the tracer happens in one of multiple ways: the tracer may itself be fluorescent, it may be radioactively tagged or conjugated with a dye or enzymatically active probe, or it may be detected via antibody binding [136]. Axonal tracing is generally performed in the living brain, after which the animal is sacrificed to detect where the tracer has ended up, but some substances also enable tracing in postmortem tissue and therefore even in the human brain, albeit over limited distances [137,138,139]. The method is well suited to characterizing medium-to-long-range connections such as those between cortical areas. A number of tracers, especially certain viral tracers, are transneuronal, crossing synapses and tracking polysynaptic pathways [140]. Furthermore, it is possible to perform double or even triple labeling to visualize the participation of neurons in two or more connection pathways [141]. Double labeling with retrograde tracers for instance suggests that the vast majority of cortico-cortical projection neurons in macaque visual cortex send connections either in the feedforward direction or in the feedback direction, not both, with respect to the hierarchy of visual areas [28].

Tracer injections typically cover a millimeter-scale area, so that multiple axons are traced at the same time, not individual ones. Because of the local spreading of the tracer, axonal tracing does not provide reliable information about the region immediately surrounding the injection site. An important drawback of the method is that only up to a few injections can be performed in each animal, so that data have to be combined across many animals to obtain a complete connectivity graph. This introduces inevitable inaccuracies due to inter-individual differences. Because tracers are taken up by neurons indiscriminately, conventional tracing does not allow the specific connections of separate subpopulations of neurons to be identified, let alone of individual neurons. However, over the past decades a number of viral tracing methods have been developed that trace specific molecularly marked neuronal subpopulations [136]. A modern technique uniquely labeling neurons with random RNA sequences enables high-throughput mapping of projections at the level of individual source neurons [142].

While axonal tracing traditionally only gave qualitative information about connectivity, for instance describing staining as sparse, moderate, or dense, more recently a number of groups have gone through the painstaking effort of counting the numbers of labeled cells in retrograde tracing experiments. A notable quantitative tracing data set characterizes the connectivity between a large number of areas in macaque cortex in terms of overall fractions of labeled neurons (FLN) and fractions of supragranular labeled neurons (SLN) in all source areas project-

ing to each injected target area [28,143]. SLN relates to the hierarchy of vision-related cortical areas, as feedforward projections tend to emanate from layer II/III and thus have a high SLN, while feedback projections emanate preferentially from infragranular layers and have a low SLN. A similarly comprehensive resource of quantitative retrograde tracing data is available for the marmoset neocortex [144,145].

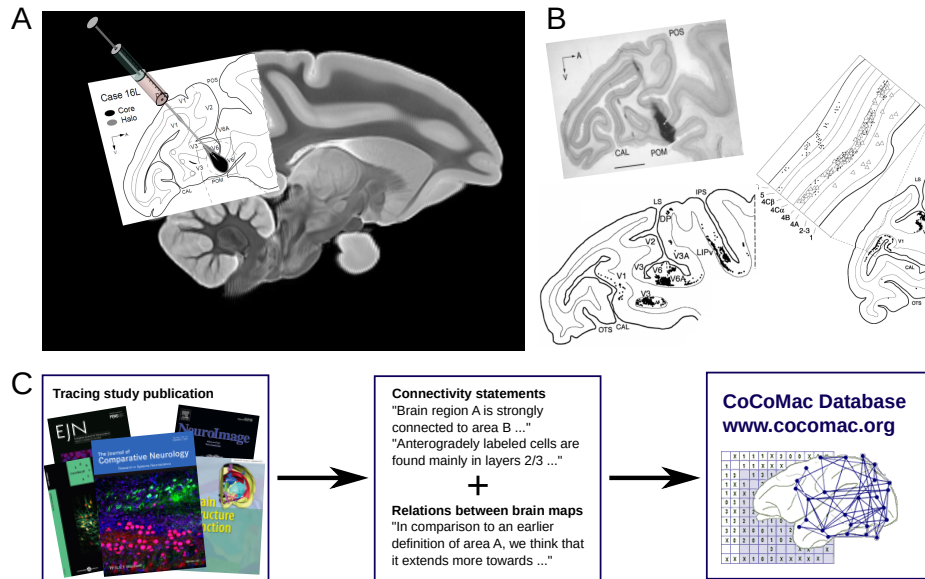


Figure 2. Workflow from tracing experiment to entry in the CoCoMac database. **A.** A tracing study is performed to study a particular part of the brain, by injecting a tracer substance into a target area. Shown is Case 16L from Galletti et al. [146], here registered to the macaque atlas of Calabrese et al. [29] via the Scalable Brain Atlas [35]. **B.** Tracer is picked up by axons, and depending on the substance it is either transported anterogradely towards the axon terminals, or retrogradely to the cell bodies, or both. After sacrificing the animal, a careful investigation of labeled cell bodies and/or axon terminals across the brain is carried out, sometimes including layer-specific quantitative data. **C.** After the results have been written up and subject to peer review, collators from the CoCoMac database take out statements on connectivity and the definitions of brain areas.

The CoCoMac database, which stands for Collation of Connectivity data on the Macaque brain [76,147], contains both anterograde and retrograde tracing data from a large number of published studies, especially for the cerebral cortex, in part with laminar resolution. Figure 2 illustrates the prerequisites for creating such a database. Another collation effort [148] has reconstructed the area-level structural connectome of the cat from qualitative axonal tracing data. The Allen Institute provides an anterograde tracing data set encompassing hundreds of

injections throughout the mouse brain [149]. A comprehensive characterization of laminar target patterns of connections between cortical areas in primate is missing to date.

Axonal tracing is a reliable method for identifying actual connection pathways, and often serves as the ground truth for evaluating diffusion tensor imaging results (cf. section 3.5). However, the fact that connectomes based on tracing data are a composite of connectivity in many individuals warrants special caution in their interpretation. The average or union of the connections in many brains in all likelihood does not accurately represent the connectivity of any individual brain.

3.5 Diffusion tensor imaging (DTI)

Diffusion tensor imaging (DTI) is a form of diffusion MRI or diffusion-weighted imaging (DWI), which measures the local rate of water diffusion at a resolution of typically a few millimeters. DTI detects anisotropies in the diffusion of water by using several different orientations of the magnetic field gradients to obtain information about the directionality of the diffusion in each voxel [150]. Since the diffusion is greater along than perpendicular to myelinated axons, the method enables the main local orientation of axonal fiber tracts to be identified. The paths of the fiber tracts maximally consistent with the local orientations are reconstructed using so-called tractography. The density of these ‘streamlines’ is a measure of connectivity between distant brain regions, and can for instance be summed within cortical areas to obtain an area-level cortical connectivity map. DTI is non-invasive and can reveal the connectivity of the whole brain at once. However, apart from possible directional specificity introduced by the choice of seed points for tractography, the connectivity provided by DTI is symmetric, as it can resolve the orientation but not the direction of fiber tracts. While most cortical inter-area projections are reciprocal with positively correlated connection density in the two directions [143,151,145], a proportion of connections is asymmetric, and these asymmetries are hereby missed. Such asymmetries are likely to be important for the dynamics predicted from neuronal network models [152]. Further drawbacks of DTI are its lack of laminar resolution and its inability to distinguish fibers with different orientations in the same voxel, such as crossing or touching (‘kissing’) fibers. Local tractographic errors due to kissing or crossing fibers add up over distance, limiting the reliability of the resulting connectivity maps, especially giving many false positives for long-distance connections [153].

The Human Connectome Project provides high-resolution preprocessed human diffusion MRI data for > 1100 subjects. Tractography was performed on an earlier, smaller data set from the Human Connectome Project and the resulting connectome was made available via the Brainnetome Atlas [16]. Prominent DTI connectomes for the macaque and mouse brains were published by Duke University [29,154].

As yet, there is no straightforward way to derive fully reliable and accurate connectomes from DTI. The same holds more generally for all the types of connectivity information we have discussed. All experimental connectivity data

have ‘gaps’: they only cover a certain spatial scale, they represent a subsample or lack precision at the given scale, or additional information is required to turn the experimental values into numbers of synapses. For this reason, methods are needed for filling in the gaps in the data in order to fully specify network models. This is the topic of the next section.

4 Predictive connectomics

Where the experimental connectivity data have gaps, we can try to fill these in using statistical estimates based on relationships of the known connectivity with properties such as cytoarchitecture or distance between brain regions. We refer to this approach as ‘predictive connectomics’. Such statistical estimates still tend to have a high degree of uncertainty associated with them, but if we want to fully define a network model, there is no way around making certain assumptions and approximations. From another perspective, the statements of predictive connectomics represent formalized hypotheses for further anatomical studies. The spatial and temporal organization of neurodevelopment simultaneously explains many empirical relationships between connectivity and other structural properties of the brain. In the present section, we discuss the major heuristics for predicting connectivity, including Peters’ rule, architectural principles, and methods based on distance and network topology, and describe how developmental origins form a common denominator for many of these heuristics. Finally, we touch upon the inference of structural connectivity from activity data.

4.1 Peters’ rule

Peters’ rule postulates that proximity between neurites (i.e. presynaptic axons and postsynaptic dendrites) can predict neuronal connectivity. It was originally proposed by Peters and Feldman (1976) [155] for the projections from the lateral geniculate nucleus to the visual cortex of the rat. The term ‘Peters’ rule’ was later coined by Braitenberg and Schüz (1991) [156], who also generalized this idea beyond the particular case studied by Peters and Feldman. The rule has since been widely used by researchers. Over time its application has varied. Rees et al. (2017) [157] reviewed the relevant literature and distinguished between three conceptually different usages of the rule, which correspond to increasing level of detail (illustrated in figure 3):

1. Population level. In the original formulation, the rule was applied as a predictor of connectivity between populations of neurons of the same type. Consider a group of neurons A (for example in the thalamus) projecting to a region containing another group B (for example pyramidal cells in visual cortex), where all neurons within the groups are of the same type. According to the original rule, the number of synapses between A and B is correlated with the spatial overlap of presynaptic axons of population A and postsynaptic dendrites of population B.

2. Single-neuron level. Extending the example from the previous point, take two neurons a_i and b_j from populations A and B, respectively. In this formulation, the probability p_{ij} for a connection between a_i and b_j to exist is proportional to the spatial proximity between their respective pre- and postsynaptic arbors.
3. Subcellular level. At the subcellular level, Peters' rule has been used to link the number of axonal-dendritic appositions to the number of synapses, regardless of cell types.

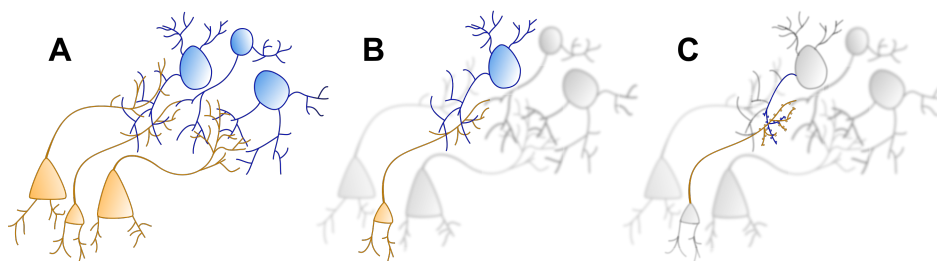


Figure 3. Illustration of the different levels of detail in the usage of Peters' rule, as described in [157]. **A.** Population level, **B.** Single-neuron level and **C.** Subcellular level.

Peters' rule is not universal and has been shown to hold for certain cases and fail in others, for all levels of detail. Section 3.1 describes an exception to Peters' rule at the subcellular level, which probably carries over to the single-neuron level as well: an apposition is more likely to predict a synapse if other synapses are present on the same neurites [114]. Other studies have provided evidence both in favor of and against the heuristic at the subcellular level [158,159,160,115]. Neurite proximity is undeniably a necessary condition for the formation of synapses, but in general not sufficient to explain it, for instance as activity-dependent plasticity may support preferential connectivity between neurons with similar response properties. Nevertheless, Peters' rule is a decent heuristic at the population level, with the main caveat that some cell types do not connect to each other even if they come into close proximity [106,157]. Thus, the rule may be fruitfully applied at the population level as long as such cell-type-specific absence of connections is taken into account.

4.2 Architectural principles

The cytoarchitecture and laminar composition of cortical areas are predictive of their connectivity, as first noted for frontal areas of macaque cortex [161,64]. In particular, architecturally more similar areas are more likely to be connected, and if they are connected, the connection density tends to be higher [162,151,45,163]. However, while architectural similarity reliably predicts the existence and ab-

sence of connections, connection densities are better explained by inter-area distances (cf. section 4.3) [162]. The characterization of areal architecture in terms of laminar differentiation was systematized using the notion of architectural types, which also consider the thickness of layer IV [65]. Areas with low architectural type have low neuron density, a thin or absent layer IV, and indistinct lamination. Areas with high architectural type have high neuron density, a thick layer IV, and distinct lamination. The progression from low to high architectural types roughly corresponds to the inverse of cortical hierarchies, down from limbic to early sensory areas. Instead of using architectural types, which discretize what is in fact a continuum of structural features across areas [164], one may use neuron density as a continuous explanatory variable. However, compared to neural density differences, architectural type differences are a better predictor of the existence and absence of connections between macaque visual areas [45].

Besides correlating with the existence or absence of connections and with connection density, architectural differences are informative of laminar projection patterns. Cytoarchitectonic difference is the only consistent predictor that explains the majority of the variance in laminar source patterns when compared with other candidate explanatory variables such as rostrocaudal distance [165]. Areas with more distinctive layers and higher neuron density tend to send projections from their upper (supragranular) layers to areas with less distinctive layers and lower neuron density. Reversely, projections from the latter to the former type of areas tend to emanate from the lower (infragranular) layers. These patterns seem to generalize across species, having already been demonstrated for cat, marmoset, and macaque [166]. Since laminar origin patterns are correlated with laminar termination patterns, for instance supragranular projections tend to target the granular layer IV [167], also termination patterns can be in part inferred from architectural similarity [151,46]. However, as the majority of layer-resolved axonal tracing data is retrograde, origin patterns have been more extensively studied than termination patterns. For human cortex, laminar origin and termination patterns of inter-area projections are still mostly unknown. For modeling purposes, the relationships between laminar patterns and cytoarchitectural differences between areas that have been observed in different mammalian species may be used to assign laminar patterns to human connectomes (figure 4).

Cortical thickness similarity has also been investigated as an explanatory variable for inter-area connectivity. Areas with more similar thickness are more likely to be connected, although this relationship does not hold consistently [45]. Thickness differences also relate to laminar patterns: projections from thinner to thicker areas tend to have a more supralaminar origin [163]. The fact that cortical thickness is somewhat predictive of connectivity fits with the observation that cortical thickness correlates negatively with neuron density [163,46]. However, compared to cortical thicknesses, architectural types and neuron densities are more systematically related to connectional features, indicating that cytoarchitecture is at the heart of the relation between cortical thickness and connectivity. More commonly, thickness similarity has been characterized in the sense of co-variation across subjects, areas with positively co-varying thicknesses

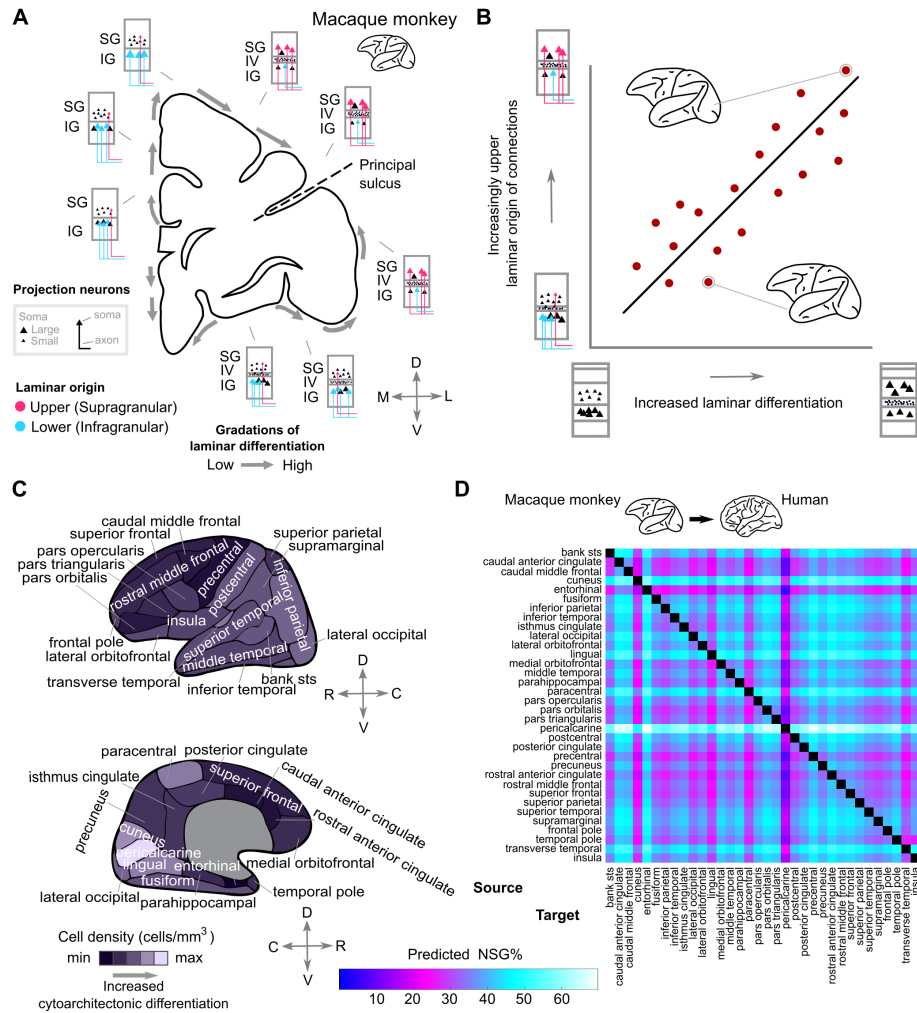


Figure 4. Laminar origin of connections, cytoarchitecture, and predictive connectomics. **A.** Laminar origin of connections shifts from lower to upper layers across the cortical sheet of the macaque monkey. **B.** Schematic illustration of the quantitative relation between the cytoarchitecture of cortical areas and the laminar origin of their connections to other areas. The transition from less to more laminar differentiation (horizontal axis), associated also with increased neural density, is accompanied by a transition of predominantly lower to upper laminar origin of connections (vertical axis). **C.** Cell densities of human cortical areas based on von Economo and Koskinas, 1925 [22]. Top, lateral view and bottom, medial view of the right hemisphere. **D.** A monkey-to-human prediction of laminar origin of connections (NSG%, relative number of supragranular neurons) between all pairs of cortical areas based on human cell densities (Panel C) and the relationship between cytoarchitecture and the laminar origin of connections (Panel B). Panel A based on a drawing from [168]. Panels C and D reproduced from [165].

across subjects being more likely to be connected [169,170,171]. However, also this correlation is far from perfect, and a large percentage of regions have co-varying thickness without being connected [170].

4.3 Distance dependence

Both for connectivity between neurons within a given brain region and for that between brain regions, shorter connections are more likely or more numerous than longer ones. This rule makes sense considering the material and energetic cost of wiring and the space taken up by axons and axon bundles. Nevertheless, non-random long-range connections between specific regions exist, which are in part explained by spatiotemporal patterns of brain development (cf. section 4.5). Locally within cortical areas, connection probability of both excitatory and inhibitory neurons falls off approximately exponentially with intersomatic distance with a space constant around $150 - 300 \mu\text{m}$ [126,127,172,173]. Besides these local connections, pyramidal cells establish patchy connectivity at distances on the scale of millimeters [174].

Similarly to local connectivity, projections between cortical areas follow an ‘exponential distance rule’ in which the lengths of axons are exponentially distributed and the probability for a neuron to send a projection between cortical areas thus falls off exponentially with distance [175]. This exponential distance rule at the level of individual neurons translates into an exponential decay in connection density at the level of areas as well [46]. Given the connectivity between cortical areas, the spatial arrangement of areas in the brain to a good approximation minimizes the total wiring length [176,177,175]. In a study of the connectivity between macaque cortical areas [143], the combination of the log ratio of neuron densities and Euclidian distance between areas provided the best statistical predictions of the existence of connections [163]. All in all, physical distance constitutes a useful explanatory variable for the existence and density of both local and long-range connectivity.

4.4 Connectome topology

So far we have considered connectivity predictions based on the properties of pairs of network nodes (neurons or areas). It is possible to go beyond pairwise properties and look at patterns of three or more nodes to infer connectivity. According to the homophily principle—described in social network theory as ‘the tendency to choose as friends those similar to oneself’ [178]—nodes with common neighbors are more likely to be themselves connected [179,165]. This property is for instance displayed by so-called small-world networks, in which a combination of many short-range and a few long-range connections enables any node to be reached via a small number of hops through the network. The homophily principle holds sway both at the single-neuron level and at the level of brain regions, in both vertebrate and invertebrate brains [179].

In local cortical circuits, certain connection motifs—patterns of connectivity in small groups of nodes—between three or more neurons are overrepresented

with respect to random graphs defined by pairwise connection probabilities alone [126,127]. In a study of groups of up to twelve neurons, the probability of a connection between a pair of neurons was found to increase linearly with the number of common neighbors. Through this expression of the homophily principle, cortical neurons cluster into small-world networks [127]. Furthermore, like-to-like connectivity between neurons with similar functional specificity, e.g., neurons in primary visual cortex having similar orientation preference or responding to the same type of visual stimuli [180], is an important ingredient of the local network topology [181].

At the level of brain regions, Jouve et al. [182] noticed that directly connected areas in macaque vision-related cortex have far more indirect connections between them than do unconnected areas. The author defined an index of connectivity that captures the fraction of shared first-order intermediate nodes between any two areas (Figure 5A). They found that this metric is related to the existence or absence of connections in macaque visual cortex, and used this to infer the connectivity of area pairs for which no tracing data were available. As pointed out in the study, the given indirect connectivity index cannot predict all connections accurately, but nevertheless exposes an underlying principle in the structure of the primate connectome.

We computed the index of indirect connectivity and the triadic motif counts on the tract-tracing data from macaque [143,183] and marmoset [145] monkeys, using the subgraphs without unknown connections. This analysis reveals that the motif counts, relative to random graphs defined by pairwise connection probabilities alone, have a similar structure in both primates, as shown previously [184] (Figure 5B). We also see that the index of connectivity has a large overlap for areas with and without a direct connection in both primates (Figure 5D). However, extreme values (> 0.8 and < 0.3) reliably distinguish existing connections from non-existing ones.

A combination of spatial proximity and homophily accounts for many topological characteristics of human cortical networks such as degree, clustering, and betweenness centrality distributions [185,186]. Chen et al. (2020) [187] found that adding cytoarchitectonic similarity to distance dependence and topological constraints resulted in even better predictions when applied to the macaque cortical connectome. These findings place local topology, and especially homophilic attachment, in the list of overarching properties governing neural network structure.

4.5 Neurodevelopmental underpinnings of connectivity heuristics

Many of the aforementioned connectivity heuristics can be brought together in a common developmental framework. The spatiotemporal ontogeny of the brain provides simultaneous explanations for distance-dependent connectivity, the preferential connectivity between cytoarchitectonically similar areas, and aspects of the network topology of the brain [179]. It also accounts for deviations from a simple decay in connection probability with distance. For instance,

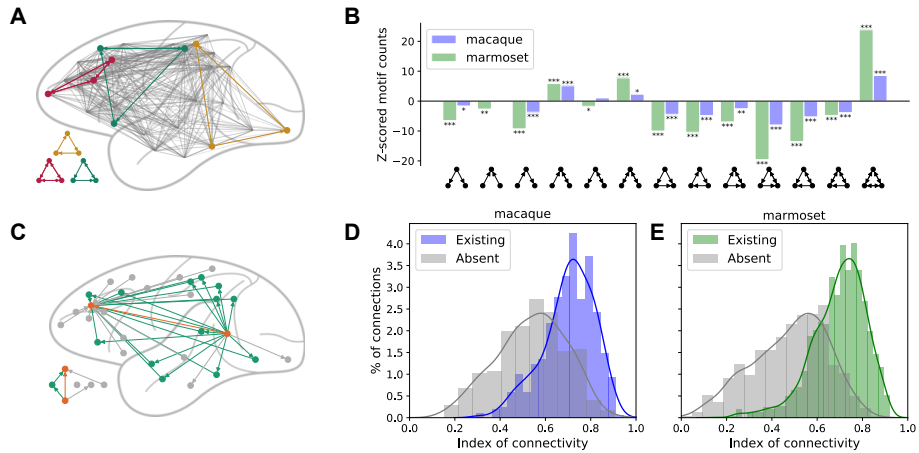


Figure 5. Illustration of topological connectivity features of macaque and marmoset cortical graphs. **A.** Schematic depiction of motifs in the area-level macaque cortico-cortical connectivity. **B.** Z-score of the motif counts for all connected triads in the macaque and marmoset. Motif counts are normalized by the mean and standard deviation of the motif counts from 1,000 random graphs with the same connection probability as the experimental data in each case; * $p < 0.05$, ** $p < 0.01$, *** $p < 0.001$. **C.** Schematic depiction of the area-level index of connectivity as described in [182]. Shared neighbors (green nodes) contribute to the prediction of a direct connection (orange), while non-shared neighbors (gray nodes) make a direct connection less likely. **D,E.** Distribution of the index of connectivity for existing and absent cortico-cortical connections in macaque (D) and marmoset (E).

changes in the parameters of the distance-dependent connectivity during development can yield a small-world network structure with multiple clusters [188]. Limbic cortical areas, of low architectural type, develop earlier and over a shorter period than areas of high laminar differentiation such as primary visual cortex. This rapid development not only underlies the less distinct lamination and low neuron density of limbic areas, but also gives these areas a longer time window for connecting to other regions, thus supporting their coordinating role [189]. The importance of spatial embedding and heterochronicity—the existence of a sequence of developmental time windows—for brain wiring were demonstrated for species ranging from the fruit fly to the mouse, rat, macaque monkey, and human [190,179]. Thus, taking into account spatiotemporal gradients of brain development can help predict more realistic connectomes regardless of the species under investigation.

4.6 Reconstructing connectivity from activity

So far we have focused on predictive relations derived from the anatomical features of the nervous tissue. However, anatomical information is often costly to

obtain or requires invasive methods and is therefore often not available for all the different brain regions. An alternative approach is to derive neural network structure from activity data. While promising results in this direction have been obtained, this approach suffers from the drawbacks that widely different network parameters can lead to closely similar activity [191] and that the external input to the network modulates the link between structure and activity [192].

When relating activity to connectivity, we need to distinguish a few different terms. Besides structural connectivity, the topic of this chapter, there are two types of activity-dependent ‘connectivity’: so-called functional connectivity, and effective connectivity. Functional connectivity is symmetric between source and target nodes, and describes correlations between their activity. It is often used in the context of functional imaging studies to characterize the interactions between brain regions. Effective connectivity is a directed measure, describing the minimal graph that would be needed to account for the observed interactions between nodes [192]. In a stricter mathematical sense, one can define effective connectivity as the product of the structural connectivity and effective synaptic weights that depend on the activity level of the target nodes and quantify their susceptibility to increased input [193]. The same structural substrate can support different functional and effective connectivities depending on the external drive and the network state. When inferring structural connectivity from activity data, the lines between the different types of connectivity can be somewhat blurred, but it is useful to keep in mind the distinctions.

We have already discussed two physiological methods that help estimate structural connectivity at the microscopic scale: paired recordings (section 3.2) and glutamate uncaging (section 3.3). These methods provide reliable connectivity data, but are constrained to small numbers of neurons. Parallel electrophysiological recordings of up to hundreds of individual neurons are now possible for instance with Utah arrays or Neuropixels probes [194,195], and functional magnetic resonance imaging enables recording whole-brain activity, resolved into ever smaller voxels [196,197].

A number of methods have been proposed for inferring the underlying connectivity from these large-scale activity data. Time-lagged correlations between the spike trains of pairs of neurons are informative about the direction of the information flow and have been shown to be linked to the structural connectivity [198]. A few studies have used this fact to reconstruct network connectivity from parallel spike train cross-correlation histograms [199,200,201]. Pairwise correlations are shaped not only by direct connections between neurons, but also by indirect connections, the electrophysiological properties of the individual neurons, transmission delays, and the external drive to the network [202,203,204]. Given certain conditions such as stationarity and knowledge of the single-neuron electrophysiology, the structural connectivity can in principle be uniquely reconstructed from the pairwise correlation functions; that is, one can compute and thereby take into account the influence of the indirect connections and shared input [205,204,193]. In practice, biological neural networks do not fulfill ideal con-

ditions and experiments do not fully provide the required information, setting a ceiling on the accuracy of structural connectivity inferred from correlations.

Going beyond pairwise correlations, Casadiego et al. [206] propose a method for inferring synaptic connections from the dependence of inter-spike intervals on cross-spike intervals, i.e. intervals between the spike times of different neurons. The method can successfully distinguish excitatory and inhibitory synapses, as validated with point neuron network simulations. Networks exhibiting phase-locked activity may not sufficiently explore the dynamical landscape to enable all synapses to be reconstructed. In such cases it can help to expose the network to different external driving conditions [207]. Similarly using only knowledge of the spiking activity and not requiring membrane potential traces, Zaytsev et al. [208] infer the connectivity of simulated networks of a thousand neurons using maximum likelihood estimation of a generalized linear model of the spiking activity. Such methods based on generalized linear models can work well when the activity of all neurons is recorded [209], but, like for any connectivity reconstruction method, undersampling is expected to diminish their performance.

Fitting the observed activity to a dynamical network model can be a complex and computationally intensive procedure. Structural connectivity parameters are sought that optimize a score or cost function based on some features of interest. In simulation-based methods, optimal parameter combinations can be searched via brute force [191,210], stochastic optimization techniques such as evolutionary methods [211,212,213], or plasticity rules [214]. Likelihood-based methods do not require costly simulations [215,216,217,218] and under some conditions allow straightforward optimization via gradient ascent or simplex methods. However, estimating the analytical likelihood function is a challenging task for complex models. Machine learning methods are starting to be developed that can overcome this issue and estimate parameter distributions given emergent dynamical properties of modeled networks [219,220].

All in all, establishing unequivocal links between structural connectivity and neural activity remains a major challenge in neuroscience, and structural connectivity estimates from population recordings should generally be interpreted with caution.

5 Validation of predicted connectivity

The most direct way of validating connectivity predictions is of course experimental confirmation. Barring the ideal situation where this is possible, we have a few options at our disposal for putting predictions to the test. In this context, different types of predictions exist: sometimes, a full connectome is generated, while sometimes merely statistical regularities in connectivity data are obtained. For the case of full connectomes, we can further distinguish generative models that do not directly rely on connectivity data, for instance based on distance, cytoarchitectonics, and topological constraints; and cases where gaps in connectivity data are filled in.

Where the result of the prediction is a full connectome, one can compare with experimentally obtained connectomes either edge-wise or based on graph properties such as degree distributions, clustering, modularity, characteristic path length, small worldness, or betweenness centrality [185,186]. The choice of properties to compare is nontrivial and depends on their presumed importance with regard to the scientific question. Ideally, the fitness of the generative model is quantified using a likelihood function, but where this is difficult, other objective functions may be defined [221].

In case of statistical fits to connectivity data, we can check the robustness of the predictions by determining confidence intervals for the fit parameters. When no straightforward expressions for these are available, bootstrapping provides a solution in which random data samples are drawn with replacement and the statistic of interest is computed for each sample [222]. A similar strategy can be applied when filling gaps in connectomes: leaving out part of the known data and either determining how well the predictions fit to the left-out data, or again computing graph properties and assessing their variability. Alternatively, we can add noise to the underlying data on the order of the uncertainty in the data. Depending on the case, ‘uncertainty’ in this context can for instance include experimental noise, inter-individual and inter-species variability, or uncertainty due to mapping between parcellations. Since it is in practice difficult to determine the size of the uncertainty, one can add different levels of noise to the estimated model parameters and check whether the predictions hold true even for relatively high noise levels.

Another route for testing the plausibility of connectivity predictions is to build corresponding network models, perform dynamical simulations, and compare the resulting activity with experimental activity data. Software tools supporting the systematic comparison between simulated and experimental activity data are available for both single neurons and networks of neurons [223]. This method is complicated by the fact that not only the connectivity but also the dynamical properties of the nodes (neurons or populations of neurons), the transmission delays, and the external drive contribute to the network dynamics. However, depending on the dynamical regime, network dynamics can be fairly robust to electrophysiological properties of the individual nodes [224]. The parameter space can be explored systematically via parameter scans, or in a more targeted manner via stochastic optimization. If at least some parameter settings for the nodes, delays, and external drive, consistent with biological data, can be found for which the predicted connectivity yields realistic activity, this provides some degree of validation. Stronger support is provided if the experimental activity data are no longer successfully reproduced upon changing the connectivity. Ultimately, neural network models should be consistent with both anatomical and electrophysiological properties of the brain.

6 Concluding remarks

Data on brain anatomy are increasingly made available as systematic, quantitative data sets, facilitating their use in neuronal network models. Inspired by seminal works like those of von Economo [22] and Braitenberg and Schüz [156], modern anatomists recognize the importance of systematization and quantification for informing analyses and models. Historically, much anatomical data was made available only in the natural language text of publications. On the example of tracing studies, the creators of the CoCoMac database [76] recognized the need to bring these data into a machine readable format and to create a framework for systematically mapping the parcellations mentioned in the text to different parcellations of choice when constructing connectivity maps. The modern, systematic way of publishing data is most prominently represented by large-scale initiatives like the Allen Institute for Brain Science, Janelia Research Campus, the Human Connectome Project, the Japanese Brain/MINDS project, and the European Human Brain Project. Nevertheless, there is sometimes still a disconnect between experimentalists and computational neuroscientists in terms of the formats in which the data are published. Anatomical data are still often made available as image files which require additional processing before they can flow into models, in formats specific to the discipline. An illustrative anecdote is that in 2018 Schmidt et al. [46] still obtained cortical thickness from micrographs by measuring with a ruler the distance between layer markers. One reason why modelers generally cannot use image data directly is that they tend to work with concepts like definite cortical areas and layers, rather than in a spatial continuum. These categorical concepts constitute strong hypotheses that help to reduce and interpret the data. Tables of area or laminar averages are then more useful than images. If the data are offered as images, at least scripts and documentation should be published alongside the data to enable the relevant quantities to be potentially more easily extracted. The latter approach retains flexibility with respect to particular parcellations and is future-proof as algorithms of feature extraction improve and concepts of brain organization may change over time.

We have described methods ranging from microscopy to diffusion magnetic resonance imaging for measuring connectivity. However, this list is not exhaustive and novel techniques are continuously developed. A modern technique is polarized light imaging (PLI), which measures fiber orientations in brain slices using the birefringence properties of myelin [225,226]. Three-dimensional reconstructions enable fiber tracts to be followed through the brain at a resolution of some tens of micrometers. Axons entering the white matter can be visualized with an in-plane pixel size down to the micrometer scale. An add-on to PLI, also based on transmitting polarized light through histological sections, is Diattenuation Imaging, which provides complementary information on tissue composition [227]. These methods promise new ways of determining the connectivity of neural network models.

Also in the field of predictive connectomics, our treatment of methods has not been exhaustive. Besides predictions based on the proximity of neural pro-

cesses or cell bodies, cytoarchitecture, topological constraints, and neural network activity, it is for instance possible to generate connectomes based on gene expression data [228,229,230]. Another possibility we have only briefly alluded to is a normative approach, in which the connectome is in some sense assumed to be optimal, and the implications of this assumption for connectivity are investigated [231,232]. As in so many fields of science, machine learning methods and artificial neural network models provide a promising new avenue for identifying regularities in data that help to predict connectivity.

As we have seen, connectomes for neural network models are subject to a variety of uncertainties. Each experimental method carries with it measurement errors, data from multiple individuals tend to be needed to fully specify a connectome, and in many cases the best available estimates even come from different species. We have largely skipped over the vast and difficult topic of mapping data between species. In many cases, the sobering truth is that this cannot be done in a fully principled manner. All types of uncertainties, whether due to experimental methods, individual differences, or interspecies differences, lead to uncertainties in predicted model dynamics. We have described some ways of verifying the robustness of network models to these uncertainties.

Brain models based on these statistical rules are necessarily models of an average brain. This limits their explanatory power. Not only in humans but also in other species, macroscopic features of brain dynamics, like dominant frequencies and functional connectivity, vary from individual to individual [233,234,235]. When the deviation of simulated brain activity from experimental data is of the same order as the inter-individual variability, there is nothing left to explain for this type of model. Schmidt et al. [236] illustrate this situation for the prediction of functional connectivity between areas on the basis of a spiking network model. Such observations challenge the research strategy to aggregate data from different species and individuals to arrive at a statistical model of brain structure. Progress may eventually only be possible by further constraining generic connectivity rules by anatomical data obtained from the individual delivering the brain activity data to be predicted [237].

Ultimately, the statistical descriptions we apply to summarize brain organization are not the rules by which brains are built in nature. The rules mathematically formalize the limits of our knowledge on the structure of individual brains. And using these rules is to date just the most efficient way of instantiating large-scale neuronal networks in a computer by a fully parallel process [238]. In nature brains are pre-shaped by evolution and further formed by growth rules in continuous interaction with the environment. Eventually we need to understand and formalize these more fundamental rules to grow artificial individual brains in a computer. This implies the existence of a sufficiently accurate model of the environment. Averages over such model instances then in turn need to be consistent with our former statistical descriptions of brain structure.

Nevertheless, the major short-term challenge consists in the construction of brain models encompassing different brain components, as already alluded to in the introduction of this chapter. With a few notable exceptions, until today

models of neuronal networks are usually constructed by a single researcher, often a PhD student, or small research groups. It seems likely that we have hit a complexity barrier and for this reason the complexity of the majority of models has not increased much over past decade. In order to integrate the heterogeneity of different brain areas and their multi-level hierarchical organization into a brain model will require that we learn to use models of brain components created by other researchers as building blocks.

International large-scale projects like EBRAINS have started to create the ICT infrastructure enabling the sharing and reuse of data and model components, as well as the simulation of multi-scale models and their environments. The hope is that using these infrastructures fosters the required culture of sharing and collaboration in neuroscience.

Acknowledgments

Supported by the European Union's Horizon 2020 Framework Programme for Research and Innovation under Specific Grant Agreements No. 785907 and 945539 (Human Brain Project SGA2, SGA3) and Priority Program 2041 (SPP 2041) "Computational Connectomics" of the German Research Foundation (DFG).

References

1. Cook, S.J., Jarrell, T.A., Brittin, C.A., Wang, Y., Bloniarz, A.E., Yakovlev, M.A., Nguyen, K.C., Tang, L.T.H., Bayer, E.A., Duerr, J.S., et al.: Whole-animal connectomes of both *Caenorhabditis elegans* sexes. *Nature* **571**(7763) (2019) 63–71
2. Kandel, E.R.: *In Search of Memory: The Emergence of a New Science of Mind*. WW Norton & Company, New York (2007)
3. Orban, G.A., Van Essen, D., Vanduffel, W.: Comparative mapping of higher visual areas in monkeys and humans. *Trends Cogn. Sci.* **8**(7) (2004) 315–324
4. Sereno, M.I., Tootell, R.B.: From monkeys to humans: what do we now know about brain homologies? *Curr. Opin. Neurobiol.* **15**(2) (2005) 135–144
5. Hutchison, R.M., Everling, S.: Monkey in the middle: why non-human primates are needed to bridge the gap in resting-state investigations. *Front. Neuroanat.* **6** (2012) 29
6. Jolivet, R., Schürmann, F., Berger, T.K., Naud, R., Gerstner, W., Roth, A.: The quantitative single-neuron modeling competition. *Biol. Cybern.* **99**(4-5) (2008) 417–426
7. Teeter, C., Iyer, R., Menon, V., Gouwens, N., Feng, D., Berg, J., Szafer, A., Cain, N., Zeng, H., Hawrylycz, M., Koch, C., Mihalas, S.: Generalized leaky integrate-and-fire models classify multiple neuron types. *Nat. Commun.* **9** (2018) 709
8. Talairach, J., Tournoux, P.: *Co-planar stereotaxic atlas of the human brain*. Thieme, Stuttgart (1988)
9. Lancaster, J.L., Tordesillas-Gutiérrez, D., Martínez, M., Salinas, F., Evans, A., Zilles, K., Mazziotta, J.C., Fox, P.T.: Bias between MNI and Talairach coordinates analyzed using the ICBM-152 brain template. *Human Brain Mapping* **28**(11) (2007) 1194–1205

10. Laird, A.R., Robinson, J.L., McMillan, K.M., Tordesillas-Gutiérrez, D., Moran, S.T., Gonzales, S.M., Ray, K.L., Franklin, C., Glahn, D.C., Fox, P.T., Lancaster, J.: Comparison of the disparity between Talairach and MNI coordinates in functional neuroimaging data: validation of the Lancaster transform. *NeuroImage* **51**(2) (2010) 677–683
11. Amunts, K., Lepage, C., Borgeat, L., Mohlberg, H., Dickscheid, T., Rousseau, M.É., Bludau, S., Bazin, P.L., Lewis, L.B., Oros-Peusquens, A.M., et al.: BigBrain: an ultrahigh-resolution 3D human brain model. *Science* **340**(6139) (2013) 1472–1475
12. Dickscheid, T., Haas, S., Bludau, S., Glock, P., Huysegoms, M., Amunts, K.: Towards 3D reconstruction of neuronal cell distributions from histological human brain sections. In Grandinetti, L., Joubert, G.R., Michielsen, K., eds.: *Future Trends of HPC in a Disruptive Scenario*. IOS Press (2019) 223–238
13. Amunts, K., Mohlberg, H., Bludau, S., Zilles, K.: Julich-Brain: a 3D probabilistic atlas of the human brain’s cytoarchitecture. *Science (First Release)* (2020) eabb4588
14. Zilles, K., Palomero-Gallagher, N., Schleicher, A.: Transmitter receptors and functional anatomy of the cerebral cortex. *J. Anat.* **205**(6) (2004) 417–432
15. Eickhoff, S.B., Thirion, B., Varoquaux, G., Bzdok, D.: Connectivity-based parcellation: Critique and implications. *Human Brain Mapping* **36**(12) (2015) 4771–4792
16. Fan, L., Li, H., Zhuo, J., Zhang, Y., Wang, J., Chen, L., Yang, Z., Chu, C., Xie, S., Laird, A.R., et al.: The human Brainnetome Atlas: a new brain atlas based on connectional architecture. *Cereb. Cortex* **26**(8) (2016) 3508–3526
17. Gordon, E.M., Laumann, T.O., Adeyemo, B., Huckins, J.F., Kelley, W.M., Petersen, S.E.: Generation and evaluation of a cortical area parcellation from resting-state correlations. *Cereb. Cortex* **26**(1) (2016) 288–303
18. Bohland, J.W., Bokil, H., Allen, C.B., Mitra, P.P.: The brain atlas concordance problem: quantitative comparison of anatomical parcellations. *PLOS One* **4**(9) (2009)
19. Arslan, S., Ktena, S.I., Makropoulos, A., Robinson, E.C., Rueckert, D., Parisot, S.: Human brain mapping: A systematic comparison of parcellation methods for the human cerebral cortex. *NeuroImage* **170** (2018) 5–30
20. Van Essen, D.C., Glasser, M.F.: Parcellating cerebral cortex: How invasive animal studies inform noninvasive mapmaking in humans. *Neuron* **99**(4) (2018) 640–663
21. Brodmann, K.: *Vergleichende Lokalisationslehre der Großhirnrinde in ihren Prinzipien dargestellt auf Grund des Zellenbaues*. Johann Ambrosius Barth, Leipzig (1909)
22. von Economo, C.F., Koskinas, G.N.: *Die Cytoarchitektonik der Hirnrinde des erwachsenen Menschen*. J. Springer (1925)
23. Schiffer, C., Spitzer, H., Kiwitz, K., Amunts, K., Dickscheid, T.: Deep learning speeds up gapless cytoarchitectonic mapping in the human brain. <https://www5.aievolution.com/hbm1901/index.cfm?do=abs.viewAbs&abs=1535> (2019) OHBM conference abstract.
24. Wagstyl, K., Lepage, C., Bludau, S., Zilles, K., Fletcher, P.C., Amunts, K., Evans, A.C.: Mapping cortical laminar structure in the 3D BigBrain. *Cereb. Cortex* **28**(7) (2018) 2551–2562
25. Desikan, R.S., Ségonne, F., Fischl, B., Quinn, B.T., Dickerson, B.C., Blacker, D., Buckner, R.L., Dale, A.M., Maguire, R.P., Hyman, B.T., et al.: An automated labeling system for subdividing the human cerebral cortex on MRI scans into gyral based regions of interest. *NeuroImage* **31**(3) (2006) 968–980

26. Shen, E.H., Overly, C.C., Jones, A.R.: The Allen Human Brain Atlas: comprehensive gene expression mapping of the human brain. *Trends Neurosci.* **35**(12) (2012) 711–714
27. Sunkin, S.M., Ng, L., Lau, C., Dolbeare, T., Gilbert, T.L., Thompson, C.L., Hawrylycz, M., Dang, C.: Allen Brain Atlas: an integrated spatio-temporal portal for exploring the central nervous system. *Nucleic Acids Research* **41**(D1) (2012) D996–D1008
28. Markov, N.T., Vezoli, J., Chameau, P., Falchier, A., Quilodran, R., Huissoud, C., Lamy, C., Misery, P., Giroud, P., Ullman, S., Barone, P., Dehay, C., Knoblauch, K., Kennedy, H.: Anatomy of hierarchy: Feedforward and feedback pathways in macaque visual cortex. *J. Compar. Neurol.* **522**(1) (2014) 225–259
29. Calabrese, E., Badea, A., Coe, C.L., Lubach, G.R., Shi, Y., Styner, M.A., Johnson, G.A.: A diffusion tensor MRI atlas of the postmortem rhesus macaque brain. *NeuroImage* **117** (2015) 408–416
30. Lein, E.S., Hawrylycz, M.J., Ao, N., Ayres, M., Bensinger, A., Bernard, A., Boe, A.F., Boguski, M.S., Brockway, K.S., Byrnes, E.J., et al.: Genome-wide atlas of gene expression in the adult mouse brain. *Nature* **445**(7124) (2007) 168–176
31. Dong, H.W.: The Allen reference atlas: A digital color brain atlas of the C57Bl/6J male mouse. John Wiley & Sons Inc (2008)
32. Kuan, L., Li, Y., Lau, C., Feng, D., Bernard, A., Sunkin, S.M., Zeng, H., Dang, C., Hawrylycz, M., Ng, L.: Neuroinformatics of the Allen Mouse Brain Connectivity Atlas. *Methods* **73** (2015) 4–17
33. Paxinos, G., Franklin, K.B.: Paxinos and Franklin’s The Mouse Brain in Stereotaxic Coordinates. 5 edn. Academic Press (2019)
34. Chon, U., Vanselow, D.J., Cheng, K.C., Kim, Y.: Enhanced and unified anatomical labeling for a common mouse brain atlas. *Nature Communications* **10**(1) (2019) 1–12
35. Bakker, R., Tiesinga, P., Kötter, R.: The Scalable Brain Atlas: Instant web-based access to public brain atlases and related content. *Neuroinformatics* **13** (2015) 353–366
36. Schiffer, C., Kiwitz, K., Amunts, K., Dickscheid, T.: Ultrahigh resolution 3D cytoarchitectonic map of Area hOc1 (V1, 17, CalcS) created by a Deep-Learning assisted workflow [Data set]. Human Brain Project Neuroinformatics Platform (2019) DOI: 10.25493/DGEZ-Q93.
37. Fischl, B., Dale, A.M.: Measuring the thickness of the human cerebral cortex from magnetic resonance images. *Proc. Natl. Acad. Sci. USA* **97**(20) (September 2000) 11050–11055
38. Lüsebrink, F., Wollrab, A., Speck, O.: Cortical thickness determination of the human brain using high resolution 3 T and 7 T MRI data. *NeuroImage* **70** (2013) 122–131
39. Cardinale, F., Chinnici, G., Bramerio, M., Mai, R., Sartori, I., Cossu, M., Russo, G.L., Castana, L., Colombo, N., Caborni, C., et al.: Validation of FreeSurfer-estimated brain cortical thickness: comparison with histologic measurements. *Neuroinformatics* **12**(4) (2014) 535–542
40. Wagstyl, K., Lerch, J.P.: Cortical thickness. In: *Brain Morphometry*. Springer (2018) 35–49
41. Li, D., Zavaglia, M., Wang, G., Xie, H., Hu, Y., Werner, R., Guan, J.S., Hilgetag, C.C.: Discrimination of the hierarchical structure of cortical layers in 2-photon microscopy data by combined unsupervised and supervised machine learning. *Scientific Reports* **9**(1) (2019) 1–16

42. Von Economo, C.: Cellular Structure of the Human Cerebral Cortex. Karger Medical and Scientific Publishers (2009) Translated and edited by L.C. Triarhou.
43. Wagstyl, K., Larocque, S., Cucurull, G., Lepage, C., Cohen, J.P., Bludau, S., Palomero-Gallagher, N., Lewis, L.B., Funck, T., Spitzer, H., et al.: BigBrain 3D atlas of cortical layers: Cortical and laminar thickness gradients diverge in sensory and motor cortices. *PLOS Biol.* **18**(4) (2020) e3000678
44. Alvarez, I., Parker, A.J., Bridge, H.: Normative cerebral cortical thickness for human visual areas. *NeuroImage* **201** (2019) 116057
45. Hilgetag, C.C., Medalla, M., Beul, S.F., Barbas, H.: The primate connectome in context: Principles of connections of the cortical visual system. *NeuroImage* **134** (2016) 685–702
46. Schmidt, M., Bakker, R., Hilgetag, C.C., Diesmann, M., van Albada, S.J.: Multi-scale account of the network structure of macaque visual cortex. *Brain Struct. Func.* **223**(3) (April 2018) 1409–1435
47. Cahalane, D., Charvet, C., Finlay, B.: Systematic, balancing gradients in neuron density and number across the primate isocortex. *Front. Neuroanat.* **6** (2012) 28
48. Pagani, M., Damiano, M., Galbusera, A., Tsaftaris, S.A., Gozzi, A.: Semi-automated registration-based anatomical labelling, voxel based morphometry and cortical thickness mapping of the mouse brain. *J. Neurosci. Methods* **267** (2016) 62–73
49. Feo, R., Giove, F.: Towards an efficient segmentation of small rodents brain: a short critical review. *J. Neurosci. Methods* (2019) 82–29
50. West, M.J.: New stereological methods for counting neurons. *Neurobiol. Aging* **14**(4) (1993) 275–285
51. Miller, D.J., Balaram, P., Young, N.A., Kaas, J.H.: Three counting methods agree on cell and neuron number in chimpanzee primary visual cortex. *Front. Neuroanat.* **8** (2014) 36
52. Herculano-Houzel, S., Lent, R.: Isotropic fractionator: a simple, rapid method for the quantification of total cell and neuron numbers in the brain. *J. Neurosci.* **25**(10) (2005) 2518–2521
53. West, M., Slomianka, L., Gundersen, H.J.G.: Unbiased stereological estimation of the total number of neurons in the subdivisions of the rat hippocampus using the optical fractionator. *The Anatomical Record* **231**(4) (1991) 482–497
54. Sterio, D.: The unbiased estimation of number and sizes of arbitrary particles using the disector. *J. Microsc.* **134**(2) (1984) 127–136
55. Mullen, R.J., Buck, C.R., Smith, A.M.: NeuN, a neuronal specific nuclear protein in vertebrates. *Development* **116**(1) (1992) 201–211
56. Merker, B.: Silver staining of cell bodies by means of physical development. *J. Neurosci. Methods* **9**(3) (1983) 235–241
57. Erö, C., Gewaltig, M.O., Keller, D., Markram, H.: A cell atlas for the mouse brain. *Front. Neuroinform.* **12** (2018) 84
58. Herculano-Houzel, S., Mota, B., Lent, R.: Cellular scaling rules for rodent brains. *Proc. Natl. Acad. Sci. USA* **103**(32) (2006) 12138–12143
59. Azevedo, F.A.C., Carvalho, L.R.B., Grinberg, L.T., Farfel, J.M., Ferretti, R.E.L., Leite, R.E.P., Filho, W.J., Lent, R., Herculano-Houzel, S.: Equal numbers of neuronal and nonneuronal cells make the human brain an isometrically scaled-up primate brain. *J. Compar. Neurol.* **513**(5) (April 2009) 532–541
60. Herculano-Houzel, S.: The human brain in numbers: a linearly scaled-up primate brain. *Front. Hum. Neurosci.* **3** (2009) 31
61. Sarko, D.K., Catania, K.C., Leitch, D.B., Kaas, J.H., Herculano-Houzel, S.: Cellular scaling rules of insectivore brains. *Front. Neuroanat.* **3** (2009) 8

62. Herculano-Houzel, S.: The remarkable, yet not extraordinary, human brain as a scaled-up primate brain and its associated cost. *Proceedings of the National Academy of Sciences* **109**(Supplement 1) (June 2012) 10661–10668
63. Collins, C.E., Airey, D.C., Young, N.A., Leitch, D.B., Kaas, J.H.: Neuron densities vary across and within cortical areas in primates. *Proc. Natl. Acad. Sci. USA* **107**(36) (September 2010) 15927–15932
64. Barbas, H., Rempel-Clower, N.: Cortical structure predicts the pattern of cortico-cortical connections. *Cereb. Cortex* **7**(7) (1997) 635–646
65. Dombrowski, S., Hilgetag, C., Barbas, H.: Quantitative architecture distinguishes prefrontal cortical systems in the rhesus monkey. *Cereb. Cortex* **11**(10) (2001) 975–988
66. García-Cabezas, M.Á., Zikopoulos, B., Barbas, H.: The Structural Model: a theory linking connections, plasticity, pathology, development and evolution of the cerebral cortex. *Brain Struct. Func.* **224**(3) (2019) 985–1008
67. Hilgetag, C.C., Beul, S.F., van Albada, S.J., Goulas, A.: An architectonic type principle integrates macroscopic cortico-cortical connections with intrinsic cortical circuits of the primate brain. *Netw. Neurosci.* **3**(4) (2019) 905–923
68. Herculano-Houzel, S., Watson, C., Paxinos, G.: Distribution of neurons in functional areas of the mouse cerebral cortex reveals quantitatively different cortical zones. *Front. Neuroanat.* **7** (2013) 35
69. Keller, D., Erö, C., Markram, H.: Cell densities in the mouse brain: a systematic review. *Front. Neuroanat.* **12** (2018) 83
70. Meyer, H.S., Wimmer, V.C., Oberlaender, M., de Kock, C.P., Sakmann, B., Helmstaedter, M.: Number and laminar distribution of neurons in a thalamocortical projection column of rat vibrissal cortex. *Cereb. Cortex* **20**(10) (2010) 2277–2286
71. Markram, H., Muller, E., Ramaswamy, S., Reimann, M.W., Abdellah, M., Sanchez, C.A., Ailamaki, A., Alonso-Nanclares, L., Antille, N., Arsever, S., Kahou, G.A.A., Berger, T.K., Bilgili, A., Buncic, N., Chalimourda, A., Chindemi, G., Courcol, J.D., Delalondre, F., Delattre, V., Druckmann, S., Dumusc, R., Dynes, J., Eilemann, S., Gal, E., Gevaert, M.E., Ghobril, J.P., Gidon, A., Graham, J.W., Gupta, A., Haenel, V., Hay, E., Heinis, T., Hernando, J.B., Hines, M., Kanari, L., Keller, D., Kenyon, J., Khazen, G., Kim, Y., King, J.G., Kisvarday, Z., Kumbhar, P., Lasserre, S., Bé, J.V.L., Magalhães, B.R., Merchán-Pérez, A., Meystre, J., Morrice, B.R., Muller, J., Muñoz-Céspedes, A., Muralidhar, S., Muthurasa, K., Nachbaur, D., Newton, T.H., Nolte, M., Ovcharenko, A., Palacios, J., Pastor, L., Perin, R., Ranjan, R., Riachi, I., Rodríguez, J.R., Riquelme, J.L., Rössert, C., Sfyrikis, K., Shi, Y., Shillcock, J.C., Silberberg, G., Silva, R., Tauheed, F., Telefont, M., Toledo-Rodriguez, M., Tränkler, T., Geit, W.V., Díaz, J.V., Walker, R., Wang, Y., Zaninetta, S.M., DeFelipe, J., Hill, S.L., Segev, I., Schürmann, F.: Reconstruction and simulation of neocortical microcircuitry. *Cell* **163**(2) (October 2015) 456–492
72. Braitenberg, V.: Brain size and number of neurons: an exercise in synthetic neuroanatomy. *J. Comput. Neurosci.* **10**(1) (2001) 71–77
73. Dale, A.M., Fischl, B., Sereno, M.I.: Cortical surface-based analysis: I. Segmentation and surface reconstruction. *NeuroImage* **9**(2) (1999) 179–194
74. Fischl, B., Sereno, M.I., Dale, A.M.: Cortical surface-based analysis: II: inflation, flattening, and a surface-based coordinate system. *NeuroImage* **9**(2) (1999) 195–207
75. Thompson, P.M., Toga, A.W.: A framework for computational anatomy. *Computing and Visualization in Science* **5**(1) (2002) 13–34

76. Stephan, K., Kamper, L., Bozkurt, A., Burns, G., Young, M., Kötter, R.: Advanced database methodology for the collation of connectivity data on the macaque brain (CoCoMac). *Phil. Trans. R. Soc. B* **356** (2001) 1159–1186
77. Stephan, K.E., Zilles, K., Kötter, R.: Coordinate-independent mapping of structural and functional data by objective relational transformation (ort). *Phil. Trans. R. Soc. B* **355**(1393) (2000) 37–54
78. Dräger, U., Olsen, J.F.: Ganglion cell distribution in the retina of the mouse. *Investigative Ophthalmology & Visual Science* **20**(3) (1981) 285–293
79. Stone, J., Rapaport, D.H., Williams, R.W., Chalupa, L.: Uniformity of cell distribution in the ganglion cell layer of prenatal cat retina: implications for mechanisms of retinal development. *Developmental Brain Research* **2**(2) (1981) 231–242
80. Curcio, C.A., Allen, K.A.: Topography of ganglion cells in human retina. *J. Compar. Neurol.* **300**(1) (1990) 5–25
81. Wässle, H., Grünert, U., Martin, P.R., Boycotts, B.B.: Immunocytochemical characterization and spatial distribution of midget bipolar cells in the macaque monkey retina. *Vision Research* **34**(5) (1994) 561–579
82. Euler, T., Wässle, H.: Immunocytochemical identification of cone bipolar cells in the rat retina. *J. Compar. Neurol.* **361**(3) (1995) 461–478
83. Shand, J., Chin, S.M., Harman, A.M., Moore, S., Collin, S.P.: Variability in the location of the retinal ganglion cell area centralis is correlated with ontogenetic changes in feeding behavior in the black bream, *Acanthopagrus butcheri* (Sparidae, Teleostei). *Brain, Behavior and Evolution* **55**(4) (2000) 176–190
84. Ahmad, A., Spear, P.D.: Effects of aging on the size, density, and number of rhesus monkey lateral geniculate neurons. *J. Compar. Neurol.* **334**(4) (1993) 631–643
85. Mitra, N.: Quantitative analysis of cell types in mammalian neo-cortex. *J. Anat.* **89**(Pt 4) (1955) 467–483
86. Sloper, J., Hiorns, R., Powell, T.P.S.: A qualitative and quantitative electron microscopic study of the neurons in the primate motor and somatic sensory cortices. *Phil. Trans. R. Soc. B* **285**(1006) (1979) 141–171
87. Cozzi, B., De Giorgio, A., Peruffo, A., Montelli, S., Panin, M., Bombardi, C., Grandis, A., Pirone, A., Zambenedetti, P., Corain, L., Granato, A.: The laminar organization of the motor cortex in monodactylous mammals: a comparative assessment based on horse, chimpanzee, and macaque. *Brain Struct. Func.* **222**(6) (2017) 2743–2757
88. Turner, E.C., Young, N.A., Reed, J.L., Collins, C.E., Flaherty, D.K., Gabi, M., Kaas, J.H.: Distributions of cells and neurons across the cortical sheet in Old World macaques. *Brain, Behavior and Evolution* **88**(1) (2016) 1–13
89. McDonald, A.J.: Cytoarchitecture of the central amygdaloid nucleus of the rat. *J. Compar. Neurol.* **208**(4) (1982) 401–418
90. Stepniewska, I., Kaas, J.H.: Architectonic subdivisions of the inferior pulvinar in New World and Old World monkeys. *Vis. Neurosci.* **14**(6) (1997) 1043–1060
91. Voogd, J., Glickstein, M.: The anatomy of the cerebellum. *Trends Cogn. Sci.* **2**(9) (1998) 307–313
92. Duvernoy, H.M.: *The human hippocampus: functional anatomy, vascularization and serial sections with MRI.* Springer (2005)
93. Schumann, T., Erő, C., Gewaltig, M.O., Delalondre, F.J.: Towards simulating data-driven brain models at the point neuron level on petascale computers. In Di Napoli, E., Hermanns, M.A., Iliev, H., Lintermann, A., Peyser, A., eds.: *High-Performance Scientific Computing: First JARA-HPC Symposium, JHPCS 2016, Aachen, Germany, October 4–5, 2016, Revised Selected Papers. Volume 10164.*, Springer (2017) 160–169

94. Romero-Garcia, R., Atienza, M., Clemmensen, L.H., Cantero, J.L.: Effects of network resolution on topological properties of human neocortex. *NeuroImage* **59**(4) (2012) 3522–3532
95. de Reus, M.A., Van den Heuvel, M.P.: The parcellation-based connectome: limitations and extensions. *NeuroImage* **80** (2013) 397–404
96. Pyka, M., Klatt, S., Cheng, S.: Parametric anatomical modeling: a method for modeling the anatomical layout of neurons and their projections. *Front. Neuroanat.* **8** (2014) 91
97. Anastassiou, C.A., Koch, C.: Ephaptic coupling to endogenous electric field activity: why bother? *Curr. Opin. Neurobiol.* **31** (2015) 95–103
98. Jirsa, V.K., Jantzen, K.J., Fuchs, A., Kelso, J.S.: Neural field dynamics on the folded three-dimensional cortical sheet and its forward EEG and MEG. In: *Biennial International Conference on Information Processing in Medical Imaging*, Springer (2001) 286–299
99. Hagen, E., Dahmen, D., Stavrinou, M.L., Lindén, H., Tetzlaff, T., van Albada, S.J., Grün, S., Diesmann, M., Einevoll, G.T.: Hybrid scheme for modeling local field potentials from point-neuron networks. *Cereb. Cortex* **26**(12) (October 2016) 4461–4496
100. Hagen, E., Næss, S., Ness, T.V., Einevoll, G.T.: Multimodal modeling of neural network activity: computing LFP, ECoG, EEG, and MEG signals with LFPy 2.0. *Front. Neuroinform.* **12** (2018) 92
101. Casali, S., Marengi, E., Medini, K.C., Casellato, C., D’Angelo, E.: Reconstruction and simulation of a scaffold model of the cerebellar network. *Front. Neuroinform.* **13** (2019) 37
102. Lundqvist, M., Rehn, M., Djurfeldt, M., Lansner, A.: Attractor dynamics in a modular network model of neocortex. *Network: Comput. Neural Systems* **17**(3) (January 2006) 253–276
103. Johansson, C., Lansner, A.: Imposing biological constraints onto an abstract neocortical attractor network model. *Neural Comput.* **19** (2007) 1871–1896
104. Traub, R.D., Kopell, N., Bibbig, A., Buhl, E.H., LeBeau, F.E., Whittington, M.A.: Gap junctions between interneuron dendrites can enhance synchrony of gamma oscillations in distributed networks. *J. Neurosci.* **21**(23) (2001) 9478–9486
105. DeWeerd, S.: How to map the brain. *Nature* **571**(7766) (2019) S6
106. Binzegger, T., Douglas, R.J., Martin, K.A.C.: A quantitative map of the circuit of cat primary visual cortex. *J. Neurosci.* **39**(24) (2004) 8441–8453
107. Denk, W., Horstmann, H.: Serial block-face scanning electron microscopy to reconstruct three-dimensional tissue nanostructure. *PLOS Biol.* **2**(11) (2004)
108. Denk, W., Strickler, J.H., Webb, W.W.: Two-photon laser scanning microscopy. *Science* **248** (1990) 73–76
109. Economo, M.N., Clack, N.G., Lavis, L.D., Gerfen, C.R., Svoboda, K., Myers, E.W., Chandrashekar, J.: A platform for brain-wide imaging and reconstruction of individual neurons. *eLife* **5** (2016) e10566
110. Winnubst, J., Bas, E., Ferreira, T.A., Wu, Z., Economo, M.N., Edson, P., Arthur, B.J., Bruns, C., Rokicki, K., Schauder, D., et al.: Reconstruction of 1,000 projection neurons reveals new cell types and organization of long-range connectivity in the mouse brain. *Cell* **179**(1) (2019) 268–281
111. Alonso-Nanclares, L., Gonzalez-Soriano, J., Rodriguez, J., DeFelipe, J.: Gender differences in human cortical synaptic density. *Proc. Natl. Acad. Sci. USA* **105**(38) (2008) 14615–14619

112. Alonso-Nanclares, L., Kastanauskaite, A., Rodriguez, J.R., Gonzalez-Soriano, J., DeFelipe, J.: A stereological study of synapse number in the epileptic human hippocampus. *Front. Neuroanat.* **5** (2011) 8
113. Zheng, Z., Lauritzen, J.S., Perlman, E., Robinson, C.G., Nichols, M., Milkie, D., Torrens, O., Price, J., Fisher, C.B., Sharifi, N., et al.: A complete electron microscopy volume of the brain of adult drosophila melanogaster. *Cell* **174**(3) (2018) 730–743
114. Kasthuri, N., Hayworth, K.J., Berger, D.R., Schalek, R.L., Conchello, J.A., Knowles-Barley, S., Lee, D., Vázquez-Reina, A., Kaynig, V., Jones, T.R., et al.: Saturated reconstruction of a volume of neocortex. *Cell* **162**(3) (July 2015) 648–661
115. Motta, A., Berning, M., Boergens, K.M., Staffler, B., Beining, M., Loomba, S., Hennig, P., Wissler, H., Helmstaedter, M.: Dense connectomic reconstruction in layer 4 of the somatosensory cortex. *Science* **366**(6469) (2019) eaay3134
116. Spruston, N., Jaffe, D.B.: Dendritic attenuation of synaptic potentials and currents: the role of passive membrane properties. *Trends Neurosci.* **17** (1994) 161–166
117. Murthy, V.N., Schikorski, T., Stevens, C.F., Zhu, Y.: Inactivity produces increases in neurotransmitter release and synapse size. *Neuron* **32**(4) (2001) 673–682
118. Harris, K.M., Fiala, J.C., Ostroff, L.: Structural changes at dendritic spine synapses during long-term potentiation. *Phil. Trans. R. Soc. B* **358**(1432) (2003) 745–748
119. Kwon, T., Sakamoto, M., Peterka, D.S., Yuste, R.: Attenuation of synaptic potentials in dendritic spines. *Cell Reports* **20**(5) (2017) 1100–1110
120. Rodriguez-Moreno, J., Porrero, C., Rollenhagen, A., Rubio-Teves, M., Casas-Torremocha, D., Alonso-Nanclares, L., Yakoubi, R., Santuy, A., Merchan-Pérez, A., DeFelipe, J., Lübke, J.: Area-specific synapse structure in branched posterior nucleus axons reveals a new level of complexity in thalamocortical networks. *J. Neurosci.* **40**(13) (2020) 2663–2679
121. Debanne, D., Boudkazi, S., Campanac, E., Cudmore, R.H., Giraud, P., Fronzaroli-Molinieres, L., Carlier, E., Caillard, O.: Paired-recordings from synaptically coupled cortical and hippocampal neurons in acute and cultured brain slices. *Nat. Protoc.* **3**(10) (2008) 1559
122. Berry, M., Pentreath, V.: Criteria for distinguishing between monosynaptic and polysynaptic transmission. *Brain Res.* **105**(1) (1976) 1–20
123. Sedigh-Sarvestani, M., Vigeland, L., Fernandez-Lamo, I., Taylor, M.M., Palmer, L.A., Contreras, D.: Intracellular, in vivo, dynamics of thalamocortical synapses in visual cortex. *J. Neurosci.* **37**(21) (2017) 5250–5262
124. Markram, H., Lübke, J., Frotscher, M., Roth, A., Sakmann, B.: Physiology and anatomy of synaptic connections between thick tufted pyramidal neurons in the developing rat neocortex. *J. Physiol. (Lond)* **500**(2) (1997) 409–440
125. Thomson, A.M., West, D.C., Wang, Y., Bannister, A.P.: Synaptic connections and small circuits involving excitatory and inhibitory neurons in layer 2-5 of adult rat and cat neocortex: Triple intracellular recordings and biocytin labelling in vitro. *Cereb. Cortex* **12**(9) (September 2002) 936–953
126. Song, S., Sjöström, P., Reigl, M., Nelson, S., Chklovskii, D.: Highly nonrandom features of synaptic connectivity in local cortical circuits. *PLOS Biol.* **3**(3) (2005) e68
127. Perin, R., Berger, T.K., Markram, H.: A synaptic organizing principle for cortical neuronal groups. *Proc. Natl. Acad. Sci. USA* **108**(13) (March 2011) 5419–5424

128. Kodandaramaiah, S.B., Flores, F.J., Holst, G.L., Singer, A.C., Han, X., Brown, E.N., Boyden, E.S., Forest, C.R.: Multi-neuron intracellular recording in vivo via interacting autpatching robots. *eLife* **7** (2018) e24656
129. Callaway, E.M., Katz, L.C.: Photostimulation using caged glutamate reveals functional circuitry in living brain slices. *Proc. Natl. Acad. Sci. USA* **90**(16) (August 1993) 7661–7665
130. Nikolenko, V., Poskanzer, K.E., Yuste, R.: Two-photon photostimulation and imaging of neural circuits. *Nat. Methods* **4**(11) (2007) 943–950
131. Noguchi, J., Nagaoka, A., Watanabe, S., Ellis-Davies, G.C., Kitamura, K., Kano, M., Matsuzaki, M., Kasai, H.: In vivo two-photon uncaging of glutamate revealing the structure–function relationships of dendritic spines in the neocortex of adult mice. *J. Physiol. (Lond.)* **589**(10) (2011) 2447–2457
132. Dantzker, J.L., Callaway, E.M.: Laminar sources of synaptic input to cortical inhibitory interneurons and pyramidal neurons. *Nat Neurosci* **3**(7) (2000) 701–707
133. Schubert, D., Kötter, R., Zilles, K., Luhmann, H.J., Staiger, J.F.: Cell type-specific circuits of cortical layer IV spiny neurons. *J. Neurosci.* **23**(7) (Apr 2003) 2961–2970
134. Hooks, B.M., Hires, S.A., Zhang, Y.X., Huber, D., Petreanu, L., Svoboda, K., Shepherd, G.M.G.: Laminar analysis of excitatory local circuits in vibrissal motor and sensory cortical areas. *PLOS Biol.* **9**(1) (2011) e1000572
135. Lanciego, J.L., Wouterlood, F.G.: A half century of experimental neuroanatomical tracing. *J. Chem. Neuroanat.* **42**(3) (2011) 157–183
136. Saleeba, C., Dempsey, B.R., Le, S., Goodchild, A.K., McMullan, S.: A student’s guide to neural circuit tracing. *Front. Neurosci.* **13** (2019) 897
137. Galuske, R., Schlote, W., Bratzke, H., Singer, W.: Interhemispheric asymmetries of the modular structure in human temporal cortex. *Science* **5486**(289) (2000) 1946–1949
138. Tardif, E., Clarke, S.: Intrinsic connectivity of human auditory areas: a tracing study with DiI. *Eur. J. Neurosci.* **13**(5) (2001) 1045–1050
139. Seehaus, A.K., Roebroek, A., Chiry, O., Kim, D.S., Ronen, I., Bratzke, H., Goebel, R., Galuske, R.A.: Histological validation of DW-MRI tractography in human postmortem tissue. *Cereb. Cortex* **23**(2) (2013) 442–450
140. Kuypers, H., Ugolini, G.: Viruses as transneuronal tracers. *Trends Neurosci.* **13**(2) (1990) 71–75
141. Köbbert, C., Apps, R., Bechmann, I., Lanciego, J.L., Mey, J., Thanos, S.: Current concepts in neuroanatomical tracing. *Prog. Neurobiol.* **62**(4) (2000) 327–351
142. Chen, X., Sun, Y.C., Zhan, H., Kebschull, J.M., Fischer, S., Matho, K., Huang, Z.J., Gillis, J., Zador, A.M.: High-throughput mapping of long-range neuronal projection using in situ sequencing. *Cell* **179**(3) (2019) 772–786
143. Markov, N.T., Ercsey-Ravasz, M.M., Ribeiro Gomes, A.R., Lamy, C., Magrou, L., Vezoli, J., Misery, P., Falchier, A., Quilodran, R., Gariel, M.A., Sallet, J., Gamanut, R., Huissoud, C., Clavagnier, S., Giroud, P., Sappey-Marinié, D., Barone, P., Dehay, C., Toroczkai, Z., Knoblauch, K., Van Essen, D.C., Kennedy, H.: A weighted and directed interareal connectivity matrix for macaque cerebral cortex. *Cereb. Cortex* **24**(1) (2014) 17–36
144. Majka, P., Chaplin, T.A., Yu, H.H., Tolpygo, A., Mitra, P.P., Wójcik, D.K., Rosa, M.G.: Towards a comprehensive atlas of cortical connections in a primate brain: Mapping tracer injection studies of the common marmoset into a reference digital template. *J. Compar. Neurol.* **524**(11) (2016) 2161–2181

145. Majka, P., Bai, S., Bakola, S., Bednarek, S., Chan, J.M., Jermakow, N., Passarelli, L., Reser, D.H., Theodoni, P., Worthy, K.H., et al.: Open access resource for cellular-resolution analyses of corticocortical connectivity in the marmoset monkey. *Nat. Commun.* **11**(1) (2020) 1–14
146. Galletti, C., Gamberini, M., Kutz, D.F., Fattori, P., Luppino, G., Matelli, M.: The cortical connections of area V6: an occipito-parietal network processing visual information. *Eur. J. Neurosci.* **13**(8) (2001) 1572–1588
147. Bakker, R., Thomas, W., Diesmann, M.: CoCoMac 2.0 and the future of tract-tracing databases. *Front. Neuroinform.* **6** (2012) 30
148. Scannell, J., Blakemore, C., Young, M.: Analysis of connectivity in the cat cerebral cortex. *J. Neurosci.* **15**(2) (1995) 1463–1483
149. Oh, S.W., Harris, J.A., Ng, L., Winslow, B., Cain, N., Mihalas, S., Wang, Q., Lau, C., Kuan, L., Henry, A.M., et al.: A mesoscale connectome of the mouse brain. *Nature* **508**(7495) (2014) 207–214
150. Basser, P.J., Mattiello, J., LeBihan, D.: MR diffusion tensor spectroscopy and imaging. *Biophys. J.* **66**(1) (1994) 259–267
151. Beul, S.F., Grant, S., Hilgetag, C.C.: A predictive model of the cat cortical connectome based on cytoarchitecture and distance. *Brain Struct. Func.* **220**(6) (2015) 3167–3184
152. Knock, S., McIntosh, A., Sporns, O., Kötter, R., Hagmann, P., Jirsa, V.: The effects of physiologically plausible connectivity structure on local and global dynamics in large scale brain models. *J. Neurosci. Methods* **1**(183) (2009) 86–94
153. Maier-Hein, K.H., Neher, P.F., Houde, J.C., Côté, M.A., Garyfallidis, E., Zhong, J., Chamberland, M., Yeh, F.C., Lin, Y.C., Ji, Q., et al.: The challenge of mapping the human connectome based on diffusion tractography. *Nat. Commun.* **8** (2017) 1349
154. Calabrese, E., Badea, A., Cofer, G., Qi, Y., Johnson, G.A.: A diffusion MRI tractography connectome of the mouse brain and comparison with neuronal tracer data. *Cereb. Cortex* (2015) bhv121
155. Peters, A., Feldman, M.L.: The projection of the lateral geniculate nucleus to area 17 of the rat cerebral cortex. I. General description. *J. Neurocytol.* **5**(1) (1976) 63–84
156. Braitenberg, V., Schüz, A.: *Anatomy of the Cortex: Statistics and Geometry*. Springer-Verlag, Berlin, Heidelberg, New York (1991)
157. Rees, C.L., Moradi, K., Ascoli, G.A.: Weighing the evidence in Peters’ rule: Does neuronal morphology predict connectivity? *Trends Neurosci.* **40**(2) (February 2017) 63–71
158. Packer, A.M., McConnell, D.J., Fino, E., Yuste, R.: Axo-dendritic overlap and laminar projection can explain interneuron connectivity to pyramidal cells. *Cereb. Cortex* **23**(12) (2013) 2790–2802
159. Merchán-Pérez, A., Rodríguez, J.R., González, S., Robles, V., DeFelipe, J., Larrañaga, P., Bielza, C.: Three-dimensional spatial distribution of synapses in the neocortex: a dual-beam electron microscopy study. *Cereb. Cortex* **24**(6) (2014) 1579–1588
160. Lee, W.C.A., Bonin, V., Reed, M., Graham, B.J., Hood, G., Glattfelder, K., Reid, R.C.: Anatomy and function of an excitatory network in the visual cortex. *Nature* **532**(7599) (2016) 370–374
161. Barbas, H.: Pattern in the laminar origin of corticocortical connections. *J. Comp. Neurol.* **252**(3) (1986) 415–422

162. Hilgetag, C.C., Grant, S.: Cytoarchitectural differences are a key determinant of laminar projection origins in the visual cortex. *NeuroImage* **51**(3) (2010) 1006–1017
163. Beul, S.F., Barbas, H., Hilgetag, C.C.: A predictive structural model of the primate connectome. *Sci. Rep.* **7**(43176) (2017) 1–12
164. von Economo, C.F., Van Bogaert, L.: *L’architecture cellulaire normale de l’écorce cérébrale*. Paris, Masson et Cie (1927)
165. Goulas, A., Majka, P., Rosa, M.G., Hilgetag, C.C.: A blueprint of mammalian cortical connectomes. *PLOS Biol.* **17**(3) (2019) e2005346
166. Goulas, A., Zilles, K., Hilgetag, C.C.: Cortical gradients and laminar projections in mammals. *Trends Neurosci.* **41**(11) (2018) 775–788
167. Felleman, D.J., Van Essen, D.C.: Distributed hierarchical processing in the primate cerebral cortex. *Cereb. Cortex* **1** (1991) 1–47
168. Sanides, F.: Functional architecture of motor and sensory cortices in primates in the light of a new concept of neocortex evolution. In Noback, C., Montagna, W., eds.: *The Primate Brain: Advances in Primatology*. New York, Appleton-Century-Crofts Educational Division/Meredith Corporation (1970) 137–208
169. Lerch, J.P., Worsley, K., Shaw, W.P., Greenstein, D.K., Lenroot, R.K., Giedd, J., Evans, A.C.: Mapping anatomical correlations across cerebral cortex (MACACC) using cortical thickness from MRI. *NeuroImage* **31**(3) (2006) 993–1003
170. Gong, G., He, Y., Chen, Z.J., Evans, A.C.: Convergence and divergence of thickness correlations with diffusion connections across the human cerebral cortex. *NeuroImage* **59**(2) (2012) 1239–1248
171. Alexander-Bloch, A., Giedd, J.N., Bullmore, E.: Imaging structural co-variance between human brain regions. *Nat. Rev. Neurosci.* **14**(5) (2013) 322–336
172. Packer, A.M., Yuste, R.: Dense, unspecific connectivity of neocortical parvalbumin-positive interneurons: A canonical microcircuit for inhibition? *J. Neurosci.* **31**(37) (September 2011) 13260–13271
173. Levy, R.B., Reyes, A.D.: Spatial profile of excitatory and inhibitory synaptic connectivity in mouse primary auditory cortex. *J. Neurosci.* **32**(16) (April 2012) 5609–5619
174. Voges, N., Schüz, A., Aertsen, A., Rotter, S.: A modeler’s view on the spatial structure of horizontal cortical connectivity in the neocortex. submitted (September 2008)
175. Ercsey-Ravasz, M., Markov, N.T., Lamy, C., Essen, D.C.V., Knoblauch, K., Toroczkai, Z., Kennedy, H.: A predictive network model of cerebral cortical connectivity based on a distance rule. *Neuron* **80**(1) (2013) 184–197
176. Young, M.P.: Objective analysis of the topological organization of the primate cortical visual system. *Nature* **358**(6382) (1992) 152–155
177. Klyachko, V.A., Stevens, C.F.: Connectivity optimization and the positioning of cortical areas. *Proc. Natl. Acad. Sci. USA* **100**(13) (2003) 7937–7941
178. Granovetter, M.: The strength of weak ties: A network theory revisited. *Sociological Theory* (1983) 201–233
179. Goulas, A., Betzel, R.F., Hilgetag, C.C.: Spatiotemporal ontogeny of brain wiring. *Sci. Adv.* **5**(6) (2019) eaav9694
180. Ko, H., Hofer, S.B., Pichler, B., Buchanan, K.A., Sjöström, P.J., Mrsic-Flogel, T.D.: Functional specificity of local synaptic connections in neocortical networks. *Nature* **473**(7345) (May 2011) 87–91
181. Billeh, Y.N., Cai, B., Gratiy, S.L., Dai, K., Iyer, R., Gouwens, N.W., Abbasi-Asl, R., Jia, X., Siegle, J.H., Olsen, S.R., et al.: Systematic integration of structural and

- functional data into multi-scale models of mouse primary visual cortex. *Neuron* (2020)
182. Jouve, B., Rosenstiehl, P., Imbert, M.: A mathematical approach to the connectivity between the cortical visual areas of the macaque monkey. *Cereb. Cortex* **8**(1) (1998) 28–39
 183. Mejias, J.F., Murray, J.D., Kennedy, H., Wang, X.J.: Feedforward and feedback frequency-dependent interactions in a large-scale laminar network of the primate cortex. *Sci. Adv.* **2**(11) (2016) e1601335
 184. Theodoni, P., Majka, P., Reser, D.H., Wójcik, D.K., Rosa, M.G., Wang, X.J.: Structural attributes and principles of the neocortical connectome in the marmoset monkey. *bioRxiv* (2020)
 185. Vértes, P.E., Alexander-Bloch, A.F., Gogtay, N., Giedd, J.N., Rapoport, J.L., Bullmore, E.T.: Simple models of human brain functional networks. *Proc. Natl. Acad. Sci. USA* **109**(15) (2012) 5868–5873
 186. Betzel, R.F., Avena-Koenigsberger, A., Goñi, J., He, Y., De Reus, M.A., Griffa, A., Vértes, P.E., Mišić, B., Thiran, J.P., Hagmann, P., et al.: Generative models of the human connectome. *NeuroImage* **124** (2016) 1054–1064
 187. Chen, Y., Zhang, Z.K., He, Y., Zhou, C.: A large-scale high-density weighted structural connectome of the macaque brain acquired by predicting missing links. *Cereb. Cortex* (2020) bhaa060
 188. Nisbach, F., Kaiser, M.: Developmental time windows for spatial growth generate multiple-cluster small-world networks. *Eur. Phys. J. B* **58**(2) (2007) 185–191
 189. Barbas, H., García-Cabezas, M.Á.: How the prefrontal executive got its stripes. *Curr. Opin. Neurobiol.* **40** (2016) 125–134
 190. Bayer, S.A., Altman, J.: Directions in neurogenetic gradients and patterns of anatomical connections in the telencephalon. *Prog. Neurobiol.* **29**(1) (1987) 57–106
 191. Prinz, A.A., Bucher, D., Marder, E.: Similar network activity from disparate circuit parameters. *Nat. Neurosci.* **7** (2004) 1345–1352
 192. Aertsen, A.M.H.J., Gerstein, G.L., Habib, M.K., Palm, G.: Dynamics of Neuronal Firing Correlation: Modulation of ‘Effective Connectivity’. *J. Neurophysiol.* **61**(5) (1989) 900–917
 193. van Albada, S.J., Helias, M., Diesmann, M.: Scalability of asynchronous networks is limited by one-to-one mapping between effective connectivity and correlations. *PLOS Comput. Biol.* **11**(9) (2015) e1004490
 194. Maynard, E.M., Nordhausen, C.T., Normann, R.A.: The Utah intracortical electrode array: A recording structure for potential brain-computer interfaces. *EEG Clin. Neurophysiol.* **102**(3) (March 1997) 228–239
 195. Jun, J.J., Steinmetz, N.A., et al.: Fully integrated silicon probes for high-density recording of neural activity. *Nature* **551** (2017) 232–236
 196. Zimmermann, J., Goebel, R., De Martino, F., Van de Moortele, P.F., Feinberg, D., Adriany, G., Chaimow, D., Shmuel, A., Ugurbil, K., Yacoub, E.: Mapping the organization of axis of motion selective features in human area mt using high-field fmri. *PLOS One* **6**(12) (2011) e28716
 197. De Martino, F., Zimmermann, J., Muckli, L., Ugurbil, K., Yacoub, E., Goebel, R.: Cortical depth dependent functional responses in humans at 7T: improved specificity with 3D GRASE. *PLOS One* **8**(3) (2013) e60514
 198. Ostojic, S., Brunel, N., Hakim, V.: How connectivity, background activity, and synaptic properties shape the cross-correlation between spike trains. *J. Neurosci.* **29**(33) (2009) 10234–10253

199. English, D.F., McKenzie, S., Evans, T., Kim, K., Yoon, E., Buzsáki, G.: Pyramidal cell-interneuron circuit architecture and dynamics in hippocampal networks. *Neuron* **96**(2) (October 2017) 505–520.e7
200. Pastore, V.P., Massobrio, P., Godjowski, A., Martinoia, S.: Identification of excitatory-inhibitory links and network topology in large-scale neuronal assemblies from multi-electrode recordings. *PLOS Comput. Biol.* **14**(8) (08 2018) 1–25
201. Kobayashi, R., Kurita, S., Kurth, A., Kitano, K., Mizuseki, K., Diesmann, M., Richmond, B.J., Shinomoto, S.: Reconstructing neuronal circuitry from parallel spike trains. *Nat. Commun.* **10**(1) (2019) 1–13
202. Cohen, M.R., Kohn, A.: Measuring and interpreting neuronal correlations. *Nat. Rev. Neurosci.* **14**(7) (July 2011) 811–819
203. Helias, M., Tetzlaff, T., Diesmann, M.: Echoes in correlated neural systems. *New J. Phys.* **15** (2013) 023002
204. Helias, M., Tetzlaff, T., Diesmann, M.: The correlation structure of local cortical networks intrinsically results from recurrent dynamics. *PLOS Comput. Biol.* **10**(1) (2014) e1003428
205. Grytskyy, D., Helias, M., Diesmann, M.: Reconstruction of network connectivity in the irregular firing regime. In: Proceedings 10th Göttingen Meeting of the German Neuroscience Society. (2013) 1192–1193
206. Casadiego, J., Maoutsa, D., Timme, M.: Inferring network connectivity from event timing patterns. *Phys. Rev. Lett.* **121** (Aug 2018) 054101
207. van Bussel, F., Kriener, B., Timme, M.: Inferring synaptic connectivity from spatio-temporal spike patterns. *Front. Comput. Neurosci.* **5**(3) (2011) doi:10.3389/fncom.2011.00003
208. Zaytsev, Y., Morrison, A., Deger, M.: Reconstruction of recurrent synaptic connectivity of thousands of neurons from simulated spiking activity. *J. Comput. Neurosci.* **39** (2015) 77–103
209. Gerhard, F., Kispersky, T., Gutierrez, G.J., Marder, E., Kramer, M., Eden, U.: Successful reconstruction of a physiological circuit with known connectivity from spiking activity alone. *PLOS Comput. Biol.* **9**(7) (2013) e1003138
210. Stringer, C., Pachitariu, M., Steinmetz, N.A., Okun, M., Bartho, P., Harris, K.D., Sahani, M., Lesica, N.A.: Inhibitory control of correlated intrinsic variability in cortical networks. *eLife* **5** (dec 2016) e19695
211. Druckmann, S., Banitt, Y., Gidon, A.A., Schürmann, F., Markram, H., Segev, I.: A novel multiple objective optimization framework for constraining conductance-based neuron models by experimental data. *Front. Neurosci.* **1**(1) (2007) 7–18 doi:10.3389/neuro.01/1.1.001.2007.
212. Rossant, C., Goodman, D.F., Platkiewicz, J., Brette, R.: Automatic fitting of spiking neuron models to electrophysiological recordings. *Front. Neuroinform.* **4** (2010)
213. Carlson, K., Nageswaran, J., Dutt, N., Krichmar, J.: An efficient automated parameter tuning framework for spiking neural networks. *Front. Neurosci.* **8** (2014) 10
214. Diaz-Pier, S., Naveau, M., Butz-Ostendorf, M., Morrison, A.: Automatic generation of connectivity for large-scale neuronal network models through structural plasticity. *Front. Neuroanat.* **10** (2016) 57
215. Paninski, L.: Maximum likelihood estimation of cascade point-process neural encoding models. *Network: Comput. Neural Systems* **15**(4) (2004) 243–262
216. Pillow, J.W., Paninski, L., Uzzell, V.J., Simoncelli, E.P., Chichilnisky, E.J.: Prediction and decoding of retinal ganglion cell responses with a probabilistic spiking model. *J. Neurosci.* **25**(47) (2005) 11003–11013

217. Ladenbauer, J., McKenzie, S., English, D., et al.: Inferring and validating mechanistic models of neural microcircuits based on spike-train data. *Nat. Commun.* **10**(4933) (2019)
218. René, A., Longtin, A., Macke, J.H.: Inference of a mesoscopic population model from population spike trains. *Neural Comput.* **32**(8) (2020) 1448–1498
219. Bittner, S.R., Palmigiano, A., Piet, A.T., Duan, C.A., Brody, C.D., Miller, K.D., Cunningham, J.P.: Interrogating theoretical models of neural computation with deep inference. *bioRxiv* (2019)
220. Gonçalves, P.J., Lueckmann, J.M., Deistler, M., Nonnenmacher, M., Öcal, K., Bassetto, G., Chintaluri, C., Podlaski, W.F., Haddad, S.A., Vogels, T.P., Greenberg, D.S., Macke, J.H.: Training deep neural density estimators to identify mechanistic models of neural dynamics. *bioRxiv* (2020)
221. Betzel, R.F., Bassett, D.S.: Generative models for network neuroscience: prospects and promise. *J. R. Soc. Interface* **14**(136) (2017) 20170623
222. Mooney, C.Z., Duval, R.D.: *Bootstrapping: A nonparametric approach to statistical inference.* Number 95. Sage (1993)
223. Gutzen, R., von Papen, M., Trench, G., Quaglio, P., Grün, S., Denker, M.: Reproducible neural network simulations: Statistical methods for model validation on the level of network activity data. *Front. Neuroinform.* **12** (2018) 90
224. Sahasranamam, A., Vlachos, I., Aertsen, A., Kumar, A.: Dynamical state of the network determines the efficacy of single neuron properties in shaping the network activity. *Sci. Rep.* **6**(1) (2016) 1–16
225. Larsen, L., Griffin, L.D., Gräßel, D., Witte, O.W., Axer, H.: Polarized light imaging of white matter architecture. *Microsc. Res. Techniq.* **70**(10) (2007) 851–863
226. Axer, M., Grassel, D., Kleiner, M., Dammers, J., Dickscheid, T., Reckfort, J., Hütz, T., Eiben, B., Pietrzyk, U., Zilles, K., et al.: High-resolution fiber tract reconstruction in the human brain by means of three-dimensional polarized light imaging. *Front. Neuroinform.* **5**(34) (2011)
227. Menzel, M., Axer, M., Amunts, K., De Raedt, H., Michielsen, K.: Diattenuation Imaging reveals different brain tissue properties. *Sci. Rep.* **9**(1) (2019) 1–12
228. Fornito, A., Arnatkevičiūtė, A., Fulcher, B.D.: Bridging the gap between connectome and transcriptome. *Trends Cogn. Sci.* **23**(1) (2019) 34–50
229. Barabási, D.L., Barabási, A.L.: A genetic model of the connectome. *Neuron* **105**(3) (2020) 435–445
230. Timonidis, N., Bakker, R., Tiesinga, P.: Prediction of a cell-class-specific mouse mesoconnectome using gene expression data. *Neuroinformatics* (2020) 1–16
231. Chklovskii, D.B.: Synaptic connectivity and neuronal morphology: Two sides of the same coin. *Neuron* **43** (2004) 609–617
232. Samu, D., Seth, A.K., Nowotny, T.: Influence of wiring cost on the large-scale architecture of human cortical connectivity. *PLOS Comput. Biol.* **10**(4) (2014) e1003557
233. Van Albada, S.J., Rennie, C.J., Robinson, P.A.: Variability of model-free and model-based quantitative measures of EEG. *J. Integr. Neurosci.* **6**(02) (2007) 279–307
234. Gordon, E.M., Laumann, T.O., Adeyemo, B., Petersen, S.E.: Individual variability of the system-level organization of the human brain. *Cereb. Cortex* **27**(1) (2017) 386–399
235. Xu, T., Sturgeon, D., Ramirez, J.S., Froudast-Walsh, S., Margulies, D.S., Schroeder, C.E., Fair, D.A., Milham, M.P.: Interindividual variability of func-

- tional connectivity in awake and anesthetized rhesus macaque monkeys. *Biol. Psychiatry Cogn. Neurosci. Neuroimaging* **4**(6) (2019) 543–553
236. Schmidt, M., Bakker, R., Shen, K., Bezgin, G., Diesmann, M., van Albada, S.J.: A multi-scale layer-resolved spiking network model of resting-state dynamics in macaque visual cortical areas. *PLOS Comput. Biol.* **14**(10) (2018) e1006359
237. Proix, T., Bartolomei, F., Guye, M., Jirsa, V.K.: Individual brain structure and modelling predict seizure propagation. *Brain* **140**(3) (2017) 641–654
238. Morrison, A., Mehring, C., Geisel, T., Aertsen, A., Diesmann, M.: Advancing the boundaries of high connectivity network simulation with distributed computing. *Neural Comput.* **17**(8) (2005) 1776–1801